Chapter 5: Ethanol Dry Reforming

5.1: Introduction

The dry reforming of ethanol is important because it couples a renewable feedstock such as ethanol with valorization of CO_2 which is a greenhouse gas. Thus, it is like killing two birds with one stone. Significant effort has been made towards developing catalysts and processes for this reaction. A summary of published literature is provided below:

Jie Yu et.al. [1] have reviewed dry reforming of ethanol and glycerol in a mini review. These include thermodynamics, catalysts used for the reactions with comments regarding their efficacy. They conclude that Ni based catalysts are popular because of their lower cost compared to noble metals such as Rh or Ir.

Amongst active metal components noble metals such as Rh, Ir and Pd are studied. Amongst non-noble metals Ni, Co and Cu are studied.

DFT studies indicate that energetics is more favorable on noble metals (relative to non-noble metals such as Cu) for the decomposition of ethanol to methane, which explains their higher activity [2].

Catalyst deactivation, mainly due to coking and also active metal sintering is acknowledged as the main challenge in these reactions. Promoters which provide lattice oxygen during reaction, metal support interaction between active metal and support and interaction of NiO with O vacancies of catalyst are stated as important for addressing deactivation.

Supports such as SiO_2, yttria-zirconia, alumina, ceria, magnesia, zirconia, MgO-Al_2O_3, ZrO_2-Al_2O_3 and zeolites including mesoporous silicas are reported for this reaction. There are diverse reports regarding their efficacy, which also appears to depend on the active metal. Drifa et.al. [3] have studied Rh supported on various supports and found the activity trend Rh/Ni- Al_2O_3 > Rh/ Al_2O_3 ~ Rh/MgO- Al_2O_3 > Rh/CeO_2- Al_2O_3 > Rh/ZrO_2- Al_2O_3 ~ Rh/La_2O_3- Al_2O_3. Zawadski et.al. [4] have reported the trend Ni/CeO_2> Ni/ZrO_2> Ni/MgO> Ni/ Al_2O_3 for supported Ni catalyst.

Promoters such as ceria and lanthana are reported to decrease coke formation due to decreased acidity, improved metal dispersion and oxygen mobility. Bahari et.al

[5] have attributed basicity and redox properties to improvement of performance of La doped Ni/Al_2O_3 catalysts. Fayaz et.al. [6] too studied effect of La promoter for Co/Al_2O_3 catalyst. They ascribe the 1.34-1.65 folds higher conversions to formation of $La_2O_2CO_3$ which helps activate CO_2 through oxygen vacancies. Fayaz et.al. [7] have found 3% Ce as optimal promoter content for Co/Al_2O_3 catalysts and attributed its efficacy to its high oxygen storage capacity. Bahari et.al [8] have studied Ce promoter on Ni/Al_2O_3 catalyst. They observe an increase in both ethanol and CO_2 conversions with increasing CO_2 partial pressure, which they attribute to facile reduction of NiO which leads to its increased interaction with CeO_2.

Bej et.al. [9] have studies nano-NiO/SiO_2 prepared by sol-gel technique supported on alumina for this reaction. They have varied Ni content from 5 to 15 wt% and report that the conversion of CO_2 peaks at a Ni content of 8.8%. They also report 76% conversion of CO_2 with near complete conversion of ethanol and H_2 yield 100%. Reaction condition 750^oC, CO_2/Ethanol 1.4 molar and space time 24.9 kg cat h/k mol ethanol is stated as most favorable. They attribute high dispersion of Ni to better performance of the catalyst.

Bellido et. al. [10] have studied Ni supported on yttria-zirconia. The support is prepared by polymerization method using citric acid and ethylene glycol. Conventional catalyst wherein Ni is impregnated onto the support is used as a comparative. They report 61% conversion of CO_2 at 800^oC for the former. Slower deactivation at higher temperature due to less carbon deposition. They state that oxygen vacancies could activate the oxygen of the CO_2 to facilitate oxidation of the carbon deposited on Ni. Similar results are also reported by Zawadski et.al. [4] who have compared 5% Ni supported on Al_2O_3, CeO_2, MgO and ZrO_2 which are dried at 80^oC and not calcined subsequently. They report complete reduction (98-99%) of NiO on alumina and ceria with higher dispersion in case of the latter. They report formation of solid solution between NiO and MgO in case of the MgO support with poor reducibility of NiO (46%) and temperature >1000^oC for complete reduction. Ni on zirconia shows intermediate reducibility 85%. They report lower coke formation on MgO and ZrO_2 supports and a decrease in coke formation with increase in reaction temperature. They conclude that Ni/CeO_2 is the better one amongst these catalysts.

Bahari et.al. [11] have studied Ce promote Ni/Al_2O_3 prepared by impregnation on γ-alumina. They report that ceria causes NiO to reduce at a lower temperature, improves dispersion of Ni and also minimizes catalyst deactivation due to oxygen mobility of CeO_2. They report formation of filamentous and encapsulating carbon on both catalysts.

Ji Siang et.al. [12] have also reviewed mechanisms and catalysts for dry reforming of ethanol. They point out that both acidic and basic sites form intermediates which undergo further reactions on metal sites to form the main products CO, H_2, CO_2 and CH_4. They also infer that noble metal catalysts have better C-C scission activity and also less propensity for coke formation than non-noble metal catalysts. Basic properties of catalyst for chemisorption of CO_2, promoters to improve dispersion of active metals, redox behavior of support to scavenge carbon are highlighted as important for performance.

Cao [13] and Cai [14] have studied ceria, zirconia and their combinations as supports and infer that metal support interaction, reducibility and presence of oxygen vacancies are important parameters for catalyst performance.

Decreased coke formation at elevated temperature has been reported by a number of authors viz. Bellido et.al. [10], Hu and Lu [15]. DFT studies by Zhang et.al. [16] suggest that excess hydrogen can mitigate catalyst deactivation by the hydrogenation of amorphous carbon to methane.

Patent literature shows that two commercial technologies are available for the dry reforming of methane. Linde DryRef with BASF's Nickel based Synspire catalyst [17] and Chiyoda's CT-CO2AR with their noble metal-based catalyst [18]. However, no commercial offering is available to date for either steam or dry reforming of ethanol.

Based on the information from published literature a set of mono-component, bi-component and multi-component supports constituting alumina, magnesia and zirconia were prepared. These supports contained fixed quantity of lanthana and ceria at nominal 5.4 wt% each. Nickel was impregnated onto these supports and the catalysts were studied exhaustively for the dry reforming of ethanol.

Key reactions in dry reforming [1] are:

Reactions that primarily form syngas:

$C_2H_5OH + CO_2 \rightarrow 3H_2 + 3CO$ ΔHr^0_{298K} = 296.7 kJ/mol (Dry reforming)

$C_2H_5OH \rightarrow CH_3CHO + H_2$ (Dehydrogenation) ΔHr^0_{298K} = 68.4 kJ/mol

$CH_3CHO \rightarrow CH_4 + CO$ (Decomposition) ΔHr^0_{298K} = -18.785 kJ/mol

$CH_3CHO + CO_2 \rightarrow 3CO + 2H_2$ ΔHr^0_{298K} = 228.2 kJ/mol (Dry reforming)

$C_2H_5OH \rightarrow 3H_2 + CO + C$ ΔHr^0_{298K} = 124.3 kJ/mol

$C_2H_5OH \rightarrow CH_4 + H_2 + CO$ ΔHr^0_{298K} = 49.7 kJ/mol (Decomposition)

$CH_4 + CO_2 \rightarrow 2H_2 + 2CO$ ΔHr^0_{298K} = 247.0 kJ/mol (Methane dry reforming)

Water Gas Shift:

$H_2O + CO \rightarrow H_2 + CO_2$ ΔHr^0_{298K} = -41.1 kJ/mol (Water Gas Shift)

Dehydration to ethylene:

$C_2H_5OH \rightarrow C_2H_4 + H_2O$ ΔHr^0_{298K} = 45.4 kJ/mol (Dehydration)

Methanation:

$2H_2 + 2CO \rightarrow CH_4 + CO_2$ ΔHr^0_{298K}= -247.0 kJ/mol (Methanation)

$3H_2 + CO \rightarrow CH_4 + H_2O$ ΔHr^0_{298K} = -247.0 kJ/mol (Methanation)

$4H_2 + CO_2 \rightarrow CH_4 + 2H_2O$ ΔHr^0_{298K} = -146.7 kJ/mol (Methanation)

Carbon forming reactions:

$CH_4 \rightarrow C + 2H_2$ ΔHr^0_{298K} = 74.6 kJ/mol

$H_2 + CO \rightarrow C + H_2O$ ΔHr^0_{298K} = -131.3 kJ/mol

$2H_2 + CO_2 \rightarrow C + 2H_2O$ ΔHr^0_{298K} = -90.1 kJ/mol

$C_2H_4 \rightarrow$ Polymer $\rightarrow 2C + 2H_2$

$2CO \rightarrow C + CO_2$ ΔHr^0_{298K} = -86.2 kJ/mol (Disproportionation)

The basic reactions are dry reforming of ethanol, dehydrogenation, decomposition, and dehydration of ethanol. These give rise to H_2, CO, CH_3CHO, C_2H_4, and H_2O which undergo further reactions such as dry reforming (of acetaldehyde or methane), and disproportionation of CO or WGS reaction. Methanation is a side reaction that decreases syngas yield. Reactions that form carbon are the decomposition of methane, disproportionation of CO, polymerization of ethylene and deep hydrogenation of CO or CO_2.

While the yield of H_2 and the H_2/CO mole ratio are key performance metrics, the activity and stability of the catalyst are also important considerations. Considering the large number of reactions that form the network, it is apparent that a multi-component catalyst may be required for this application.

5.2: Experimental

The dry reforming of ethanol was studied using the same set of 17 supported metal catalysts which were evaluated for steam reforming of ethanol and whose characteristics are described in Chapter 3 above. La and Ce were at fixed concentrations of nominal 5.4wt% in all 17 catalysts. In brief, these catalysts comprised:

1. Three binary supports comprising oxides of Al, Mg or Zr (and rare earths).
2. Six ternary supports which are combinations of Al and Mg or Al and Zr or Mg and Zr (and rare earths).
    a. Three ternary catalysts with balanced composition (wherein the weight per cent of the two main components is equal) of Al and Mg or Al and Zr or Al and Mg
    b. Two ternary supports each of Al-Mg or Al-Zr with composition skewed in favor of Zr or Mg
3. And three quaternary supports containing Al, Mg, and Zr with varying compositions (and rare earths).
    a. Ni content was maintained constant at nominal 7.5 wt% in the case of most of the catalysts, except the balanced Al-Mg and Al-Zr ternary catalysts. In these two latter cases, Ni content was varied over the range of 5-7.5-10 wt%.

The catalyst was sized to 0.5-1.0 mm size fraction. Reaction conditions were CO_2:Ethanol 1 Molar, atmospheric pressure, LHSV $8h^{-1}$ (on liquid feed), and Nitrogen/Ethanol 1.0 molar. The reaction temperature was studied at five levels, 550°C, 600°C, 650°C, 700°C and 750°C. Time on stream 8 hours. Select runs with ternary Al-Zr catalyst with balanced composition and quaternary catalyst rich in Mg were carried out for 80 hours on stream at 650°C and 700°C at the above conditions.

5.3: Catalyst activity and correlation with catalyst characteristics

The catalyst activity was assessed by comparing the conversion of ethanol and CO_2 at 2nd hour on stream at all temperatures. The conversion of ethanol at different reaction temperatures is given in Figure 102 below.

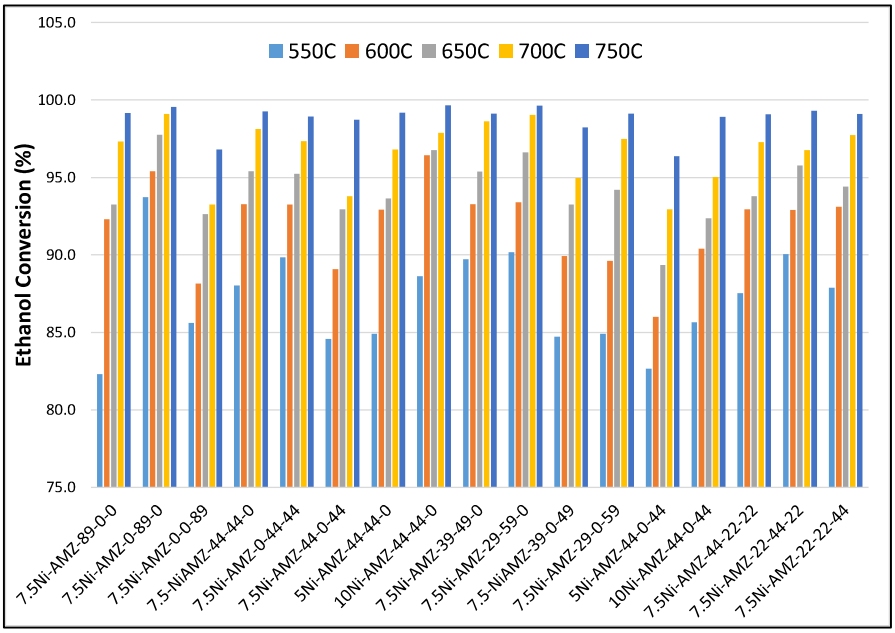

Figure 102: Ethanol Conversion at Different Temperature for EDR Reaction for various catalysts

As seen from this Figure the conversion of ethanol increases with increasing reaction temperature for all the catalysts. The trend appears to be logarithmic or polynomial. Bahari et.al [11] who have studied dry reforming of ethanol on Ce promoted Ni/Al_2O_3 catalysts report a similar increase in ethanol conversion with temperature in the range 647°C - 697°C.

The conversion at the 2nd hour at 550°C is shown in Figure 103 below. Values of an average conversion over 8 hours are also shown in this Figure.

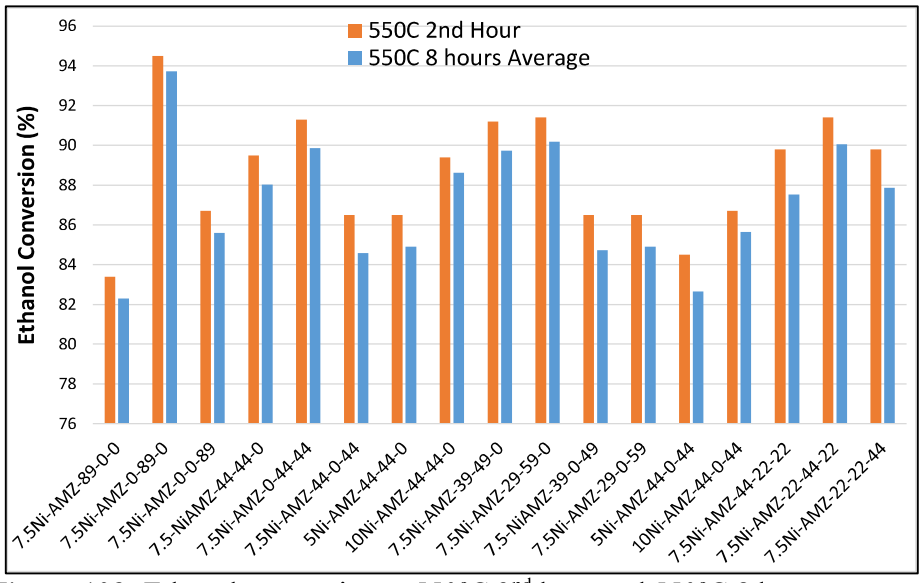

Figure 103: Ethanol conversion at 550°C 2nd hour and 550°C 8 hours average.

As seen from this Figure, the trend of activity for binary catalysts is Mg>>Zr>Al. It is also noted that the binary Mg catalyst shows the highest ethanol conversion across the entire series of catalysts studied. Zawadski et.al. [4] have reported the trend Ni/CeO_2> Ni/ZrO_2> Ni/MgO> Ni/Al_2O_3 for supported Ni catalyst. The trend in the current study is similar to that of Zawadiski's for the binary Mg and Al catalysts. However, the binary zirconia catalyst shows significantly lower activity than the magnesia catalyst in the current study. It is noted that while the catalysts of the current study are calcined at 650°C, those of Zawadski's are only dried at 80°C.

Amongst the ternary catalysts, the trend for ethanol conversion is skewed Al-Mg = balanced Mg-Zr > Balanced Al-Mg > Al-Zr. The conversion of ethanol increases with increasing Ni content for both the balanced Al-Mg (44-44-0) and balanced Al-Zr (44-0-44) series of catalysts. Since a study of Ni supported on bi-component supports is not available, comparison is made with the study of Drifa et.al [3] wherein Rh is supported on bi-component supports. The trend of activity reported is $Rh/Ni\text{-}Al_2O_3$ > Rh/Al_2O_3 ~ $Rh/MgO\text{-}Al_2O_3$ > $Rh/CeO_2\text{-}Al_2O_3$ > $Rh/ZrO_2\text{-}Al_2O_3$ ~ $Rh/La_2O_3\text{-}Al_2O_3$. Comparing the trend with respect to the supported Ni catalysts of the current study, the ternary Al-Mg catalysts show higher activity than ternary Al-Zr catalysts which is similar to that reported by Drifa et.al.

The quaternary catalysts show the trend Mg rich > Zr rich = Al rich.

Between the series the trend is Binary Mg> skewed Al-Mg = Balanced Mg-Zr= Quaternary Mg-rich > Quaternary Zr-rich = Quaternary Al-rich > Balanced Al-Mg >Balanced Al-Zr=Skewed Al-Zr. Thus, quaternary Mg-rich catalyst shows conversion comparable to skewed Al-Mg and only next to binary Mg catalyst.

The conversion at 600°C and 650°C is shown in Figure 104 below.

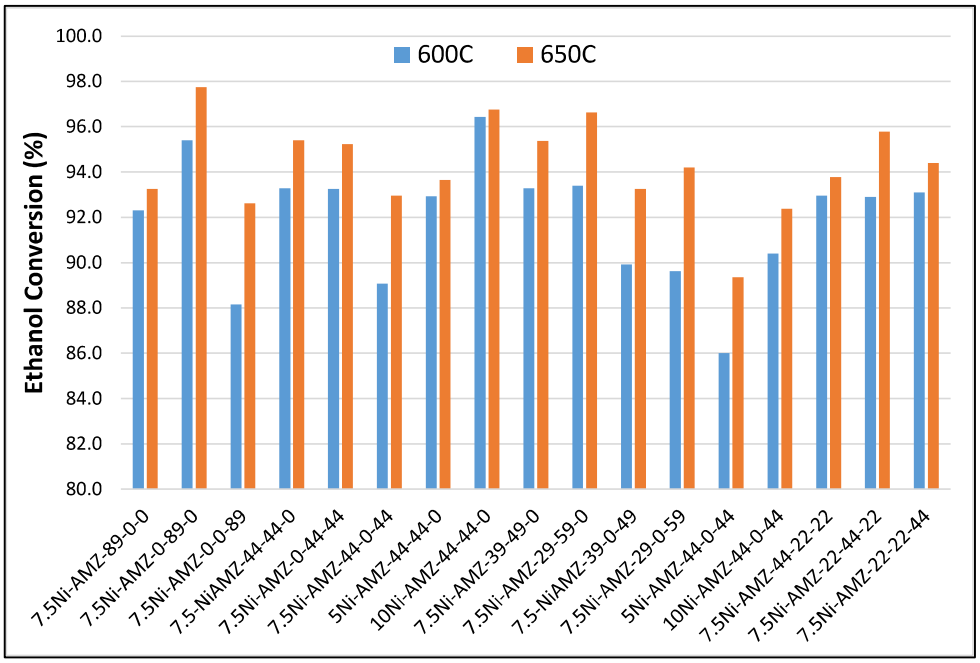

Figure 104: Ethanol conversion at 600°C and 650°C for various catalysts

As seen from this Figure the trend is largely like that of the trend at 550°C.

The trend of conversion of ethanol in EDR with catalyst composition (Figure 104) largely mimics that of ESR (Figure 54 (b)). Hence, the correlation of activity for EDR with catalyst characteristics such as catalyst composition, BET-specific surface area, the peak temperature of reduction, metal reducibility, dispersion of Ni and interaction of Ni with the specific composition of support is expected to be the same as in ESR. Hence, to avoid repetition such correlation is not made in this chapter for EDR.

The trend of conversion of CO_2 in 2nd hour with temperature is shown in Figure 105 below.

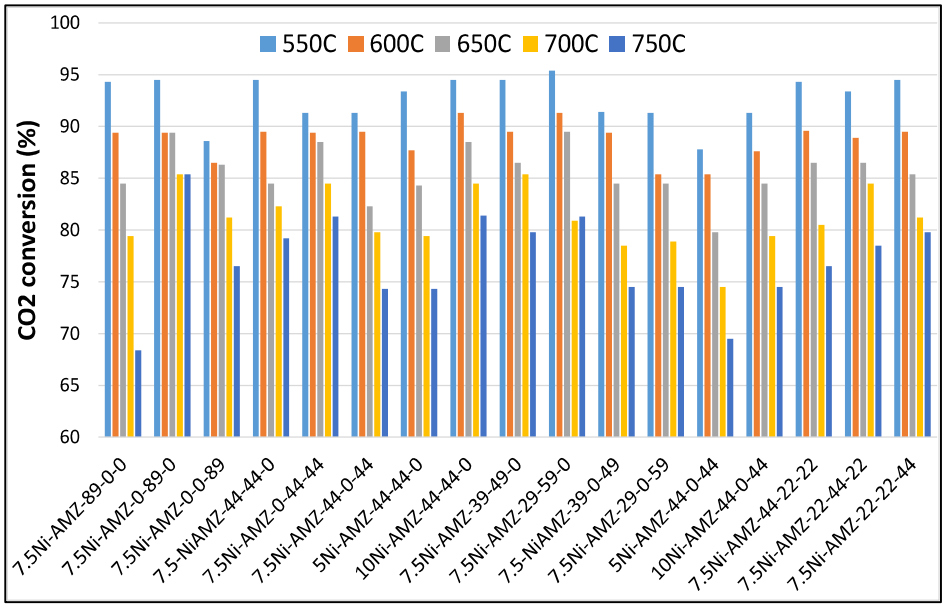

Figure 105: CO_2 conversion at various temperatures for EDR Reaction for various catalysts

As seen from this Figure all the catalysts show a decrease in conversion of CO_2 with increasing reaction temperature. The trend appears to be polynomial. It is noted from Figure 102 that the conversion of ethanol increases with temperature. This indicates that competing reactions of ethanol that do not consume CO_2 or those which produce CO_2 kick in at higher temperatures. These reactions are:

- the catalytic decomposition of ethanol (which does not consume CO_2) and produces equimolar CH_4, CO and H_2 or H_2 and CO in a molar ratio of 3:1 along with Carbon.
- the steam reforming of ethanol (source of water from dehydration of ethanol) which produces H_2 and CO_2 in a 3:1 molar ratio when there is adequate water as a reactant or produces H_2 and CO in a molar ratio 2 when water reactant is limiting. This latter reaction consumes ethanol without using CO_2 as a reactant nor does it produce CO_2 as a product)

An alternate possibility is the formation of CO_2 by reactions such as:

- steam reforming of ethanol which produces H_2 and CO_2 in a 3:1 molar ratio when adequate water is available as reactant (as explained above)
- the Water Gas Shift reaction which consumes CO to produce equimolar CO_2 and H_2

- or the disproportionation of CO ($2CO = CO_2 + Carbon$) which consumes CO and produces equimolar CO_2 and carbon.
- or the methanation of CO at hydrogen lean conditions ($2H_2 + 2CO = CO_2 + CH_4$) which produces CO_2 and CH_4.

5.4: Reaction Mechanism

Considering multiple possibilities, the comparison of derived parameters such as H_2/CO, H_2/CH_4 and $XEtOH/XCO_2$ (ratio of conversions) are useful in understanding which of the above reactions is taking place. The values of these parameters are presented in Table 8. These derived parameters are used to elicit information about the mechanism occurring on catalysts with different compositions in a subsequent section of this chapter.

As seen from the above Figure 105, the decrease of CO_2 conversion with increasing temperature is very sharp for the binary Al catalyst followed by binary Zr and ternary Al-Zr and quaternary catalysts. It is relatively less for binary Mg and ternary Al-Mg or Mg-Zr catalysts. Between the binary catalysts, Al and Mg catalysts show higher conversion of CO_2 than the Zr catalyst at 550°C and 600°C. Above this temperature, the trend is binary Mg > Zr >> Al. Amongst the ternary catalysts, there is no significant difference in conversion of CO2 with reaction temperature between balanced and skewed Al-Mg catalysts or Al-Zr catalysts. The same holds for quaternary catalysts.

The trend of conversion of CO_2 at 550°C is shown in Figure 106 below.

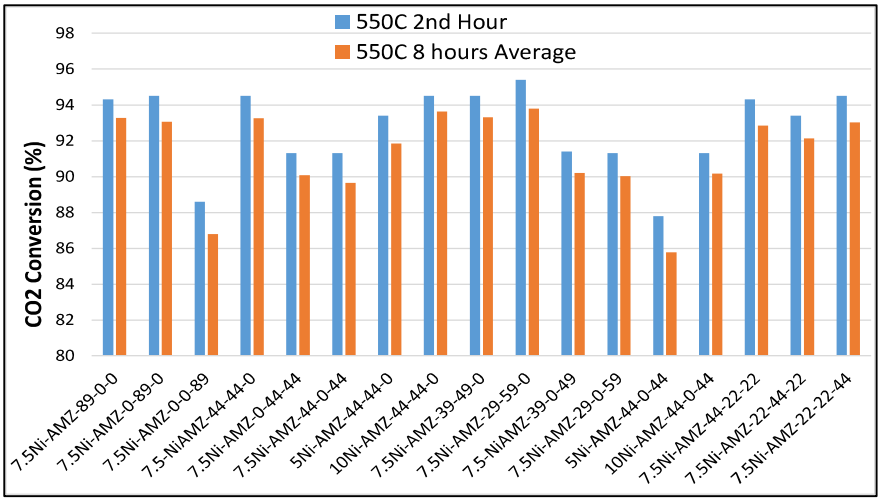

Figure 106: CO_2 conversion at 550°C temperature for various catalyst

As seen from this Figure the trend for binary catalysts is Mg=Al>>Zr. For ternary catalysts, it is Skewed Al-Mg=Balanced Al-Mg>Mg-Zr=Al-Zr. The catalysts with 5wt% Ni in both AMZ-44-44-0 and AMZ-44-0-44 series show lower conversion than the catalysts containing 7.5 or 10 wt% Ni. The trend of quaternary catalysts is Al rich=Zr rich>Mg rich.

The trend for conversion of CO_2 with respect to catalyst composition is largely like that of ethanol for the binary and ternary catalysts, whereas it is opposite that of ethanol for the quaternary catalysts. The significantly low conversion of CO_2 of binary Zr catalyst is improved by the presence of Al in ternary Al-Zr and Al and Mg in quaternary catalysts. Materials with basic character are known to adsorb CO_2 and this is used as a technique for determining basicity. Hongxue Zeng et.al [19] who have studied materials for CO_2 capture also report the same. The results of the current study are consistent with this behavior of materials with basic character.

Between the series, the trend is skewed Al-Mg≥balanced Al-Mg=Binary Mg=Binary Al=Quaternary Al=Quaternary Zr>Quaternary Mg>ternary Al-Zr=ternary Mg-Zr>binary Zr.

Similar trends are observed at higher temperatures (600°C and 650°C).

The trend of the yield of H_2 with temperature for the catalysts is shown in Figure 107 below.

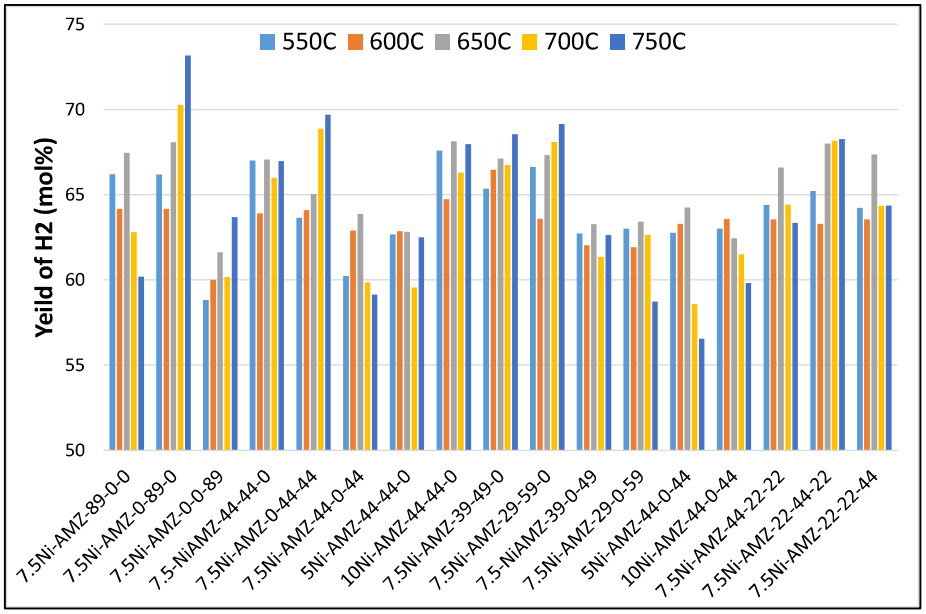

Figure 107: Yield of H_2 (mol%) at various temperature for various catalyst

As seen from this Figure, the overall trend of H_2 yield for binary catalysts is Mg>Al>Zr. For ternary catalysts, it is Skewed Al-Mg≥balanced Al-Mg=Mg-Zr>skewed Al-Zr>balanced Al-Zr. For quaternary catalysts, all three Al-rich, Mg-rich and Zr-rich show similar yields with the quaternary Mg showing higher yields at ≥650°C.

Between the series the trend is binary Mg>skewed Al-Mg≥balanced Al-Mg=balanced Mg-Zr=quaternary Mg-rich>quaternary Al or Zr>skewed Al-Zr>balanced Al-Zr>Binary Al>binary Zr.

Mixed trends are seen with temperature. Within the binary catalysts binary Al shows a decrease in yield of H_2 with increasing reaction temperature whereas binary Mg and Zr show an increase. Amongst ternary catalysts, the Al-Mg catalysts with balanced composition show an erratic trend whereas the catalysts with skewed composition show a slight increase. The ternary Al-Zr catalysts with balanced composition show a clear decrease whereas those with skewed composition show a plateau. The yield of H_2 increases with increasing Ni content for both the AMZ-44-44-0 and AMZ-44-0-44 series. The quaternary catalysts show a trend like the ternary catalysts. The Mg-rich catalyst shows an increase whereas the Al-rich or Zr-rich catalysts do not show an appreciable change with increasing reaction temperature.

The trend is very different from that obtained in ESR where the yield of H_2 increased with reaction temperature for all the catalysts. The reason for this erratic behavior appears to be the concurrent consumption of H_2 in side reactions such as methanation and its production in reactions such as WGS. This is elaborated on in the sections below.

The trend of the yield of CO is shown in Figure 108 below.

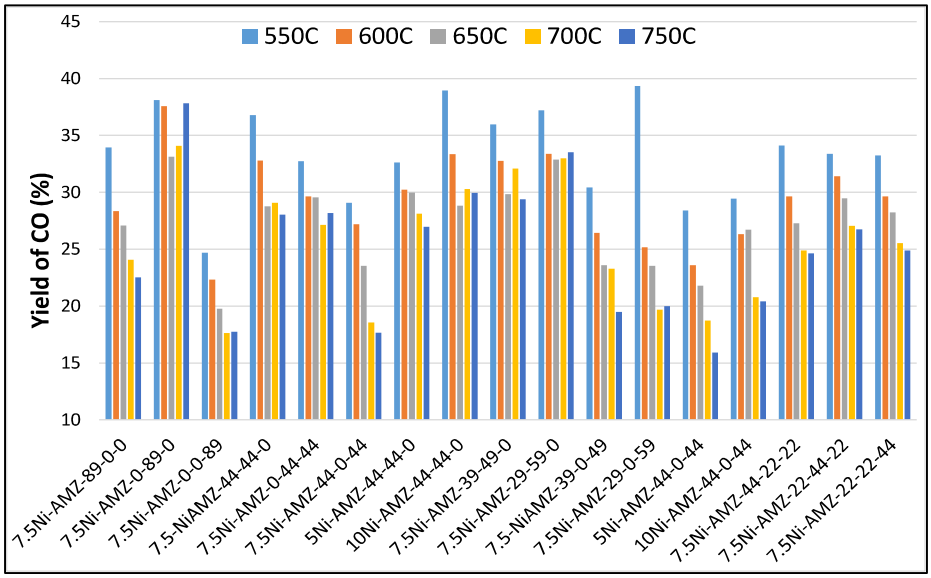

Figure 108: Yield of CO (mol%) at various temperature for various catalyst

As seen from the above Figure the trend is an exponential decrease. The trend of the value of yield of CO for binary catalysts is Mg>Al>Zr. For ternary catalysts, it is skewed Al-Mg>Balanced Al-Mg>Mg-Zr>balanced Al-Zr>skewed Al-Zr. The trend with Ni content is 10%Ni-AMZ-44-0-44>7.5%Ni-AMZ-44-0-44=5%Ni-AMZ-44-0-44 at temperature ≤650°C. A similar trend is seen for the AMZ-44-44-0 series at lower temperatures. For quaternary catalysts, all three catalysts show similar yields quaternary Mg rich=quaternary Al rich=quaternary Zr rich.

Between the series the trend is binary Mg>skewed Al-Mg>balanced Al-Mg>Mg-Zr=quaternary catalysts>binary Al>balanced Al-Zr>skewed Al-Zr>binary Zr.

The trend of the yield of CO decreases with temperature for most of the catalysts. The binary Mg and skewed Al-Mg show a relatively flat trend or parabolic trend with temperature.

Jankhah et.al [20] have simulated thermodynamic equilibrium composition in the temperature range 250°C-850°C, at $CO_2/C_2H_5OH = 1$. According to their results in the temperature range relevant to the current study 550°C-750°C: both concentrations of H_2 and CO increase whereas those of H_2O, Carbon, methane, and CO_2 decrease. They have validated their simulation by reforming ethanol on the surface of carbon steel. The authors attribute these trends to the secondary reforming of methane which is formed from the reforming of ethanol. Ethylene is not included because carbon steel does not catalyze the dehydration reaction. The results of the current study agree with

those of Jankhah et. al. [20] with respect to hydrogen and carbon (because higher temperatures show significantly slower deactivation and HRTEM does not show significant sintering of Ni). The reason appears to be poor activity of carbon steel for side reactions such as WGS, ethanol dehydration and Boudouard. Bahari et.al [8] have studied ethanol dry reforming on Ce-promoted Ni/Al_2O_3 in the temperature range 647°C -707°C. They report an increase in ethanol conversion, hydrogen yield, methane yield and H_2/CO and a decrease in CH_4/CO which is like results obtained in the current study. Thus, compared to results of Jankhah et.al., the results obtained in the current study as well as those of Bahari et.al. are strongly influenced by side reactions due to the inherent chemical activity of the catalyst. Interestingly, Shulin Zhao et.al. [21] have studied Rh/CeO_2 for dry reforming of ethanol at CO_2/C_2H_5OH =1, 1 atm, 450°C-700°C and reported a product distribution like that obtained by Jankhah et.al.[20] over carbon steel.

The effect of relevant stoichiometric reactions (which are reported to occur in EDR) on ratios H_2/CO, H_2/CH_4 and $XEtOH/XCO_2$ is compiled in Table 8 below. These are useful in identifying the individual reactions occurring on catalysts with different compositions.

Table 8: Effect of reactions on stoichiometric molar ratios of H_2/CO, H_2/CH_4 and $XEtOH/XCO_2$ in EDR Reaction.

Type	Reaction	H_2	CO	CO_2	CH_4	C_2H_4	H_2/CO	H_2/CH_4	$XEtOH/XCO_2$	C
Reforming (EDR)	$C_2H_5OH + CO_2$	3	3				1		1	
Decomposition	C_2H_5OH	1	1		1		1	1	Inc	
Decomposition	C_2H_5OH	3	1				3		Inc	1
Reforming (EDR)	$CH_4 + CO_2$	2	2				1	Inc		
WGS	$CO + H_2O$	1		1			Inc		Inc	
Dehydration	C_2H_5OH					1				
Methanation	$2H_2 + 2\ CO$			1	1		No change	Dec	Inc	
Methanation	$CO + 3H_2$				1		Dec	Dec		
Methanation	$CO_2 + 4H_2$				1			Dec	Dec	
Decomposition	CH_4	2						Inc		1
Hydrogenation	$H_2 + CO$						No change			1
Hydrogenation	$2H_2 + CO_2$						Dec		Dec	1
Disproportionation	2CO			1			Inc		Inc	1
Polymerization	n C_2H_4									1

** NOTE: Water formation is not shown in Table. Inc: Increase; Dec: Decrease.

The trend of XEtOH/XCO_2 is shown in Figure 109 below.

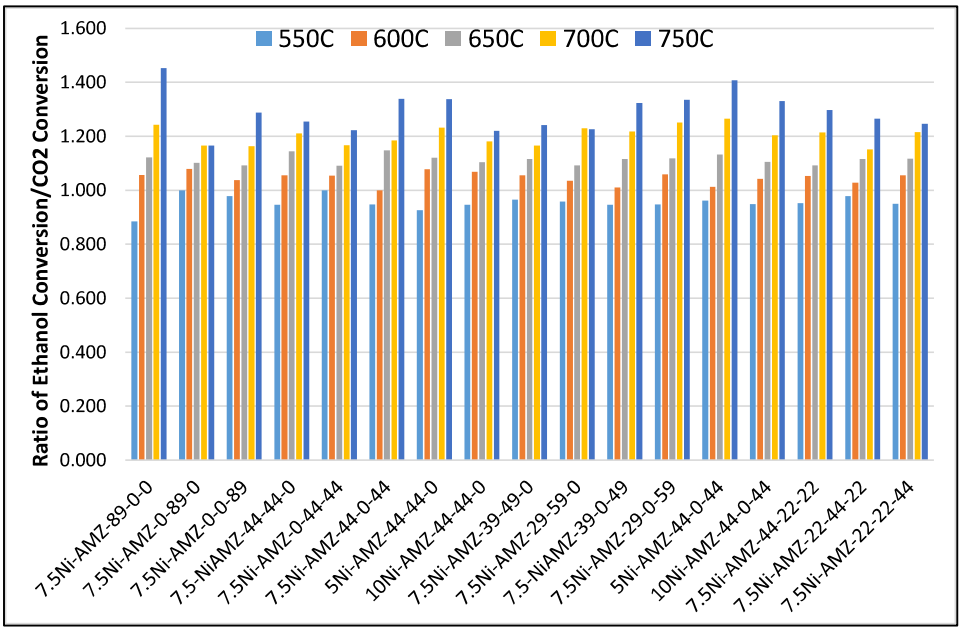

Figure 109: Trend of ratio of Ethanol Conversion/CO_2 conversion at various temperature for various catalysts.

As seen from the above Figure 109 the trend of increase in the ratio of conversion of ethanol to conversion of CO_2 with increasing temperature is close to linear. The ratio increases with increasing reaction temperature for all the catalysts. The ratio is largely in the range of 0.95 – 1.2 in runs carried out at 550°C -600°C, which is consistent with the stoichiometric molar ratio of the reactants for the main EDR reaction:

$C_2H_5OH + CO_2 \rightarrow 3H_2 + 3CO$ $\quad\quad$ $\Delta Hr^0_{298} = 296.7$ kJ/mol (Dry reforming)

It increases with further increase in reaction temperature beyond 600°C to about 1.17-1.25 for catalysts containing Mg and to about 1.32-1.4 for catalysts containing Zr. Since the conversion of ethanol increases with increasing reaction temperature over the entire range (Figure 103 and Figure 104) whereas that of CO_2 decreases (Figure 109 above), it is clear that ethanol is getting converted by other reactions such as catalytic decomposition to syngas or syngas plus methane or dehydration to ethylene which do not involve CO_2 as a reactant. This is consistent with the trend of an increase in the yield of ethylene (Figure 112) and yield of methane (Figure 114) with increasing reaction temperature.

The trend of H_2/CO (molar) is shown in Figure 110 below.

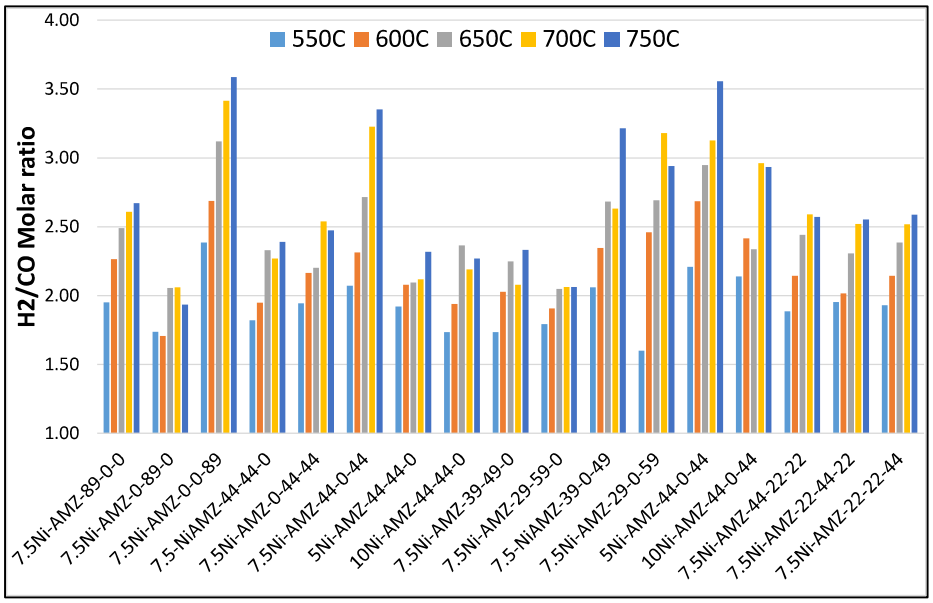

Figure 110: Trend of H_2/CO molar ratio at various temperatures for various catalysts

As seen from Figure 110 above the trend of the ratio of H_2/CO is rather linear with reaction temperature. The value of the ratio for binary catalysts is Zr>>Al>Mg. For ternary catalysts, it is Al-Zr>Mg-Zr>Al-Mg. There is no clear trend with Ni content. There is no clear trend with the composition of the quaternary catalysts. Between the series, the trend is Binary Zr >Ternary Al-Zr>Quaternary>Binary Mg = Ternary Al-Mg catalysts. H_2/CO values are lower for binary and ternary catalysts of Mg with values ranging from 1.7 to 1.9 at temperatures 550°C-600°C. The ratio increases to about 2.3-2.4 with increasing temperature. The catalysts containing Zr show values that start at about 2 and increase to 3.59 with increasing temperature for ternary Al-Zr catalysts.

The catalysts largely show an increase in the ratio of H_2/CO with increasing temperature. Bahari et.al [11] who have studied dry reforming of ethanol on Ce promoted Ni/Al2O3 catalysts report a similar increase in this ratio with temperature in the range 647°C-697°C. However, the ratio is larger in the current study. The increase is higher for binary and ternary catalysts containing Zr or Al and their combination. The binary Mg and ternary Al-Mg catalysts (which do not contain Zr) show an initial increase followed by a plateau starting at 650°C. The increase in the ratio of H_2/CO is consistent with a decrease in the yield of CO with increasing temperature (Figure 108), which could be due to its consumption by WGS or disproportionation or methanation under H_2 lean conditions. The yield of H_2 (Figure 107) shows mixed trends with no large changes with reaction temperature for most of the catalysts, whereas methanation

consumes 3 moles H_2 per mole CO, which would cause a decrease in yield of H_2. Hence methanation is an unlikely candidate among these reactions. Since the conversion of CO_2 also decreases significantly with temperature the conversion of CO by disproportionation or by WGS (which produce CO_2 as a product) are more likely candidates. Source of water would be from the dehydration of ethanol.

The trend of H_2/CH_4 with reaction temperature is shown in Figure 111 below. The trend is an exponential decrease with increasing reaction temperature. As seen from this Figure the ratio decreases sharply with increasing reaction temperature (exponential decrease). The ratio is relatively higher in the lower temperature region (550°C -600°C) for binary Zr and ternary Al-Zr catalysts when compared to the remaining catalysts.

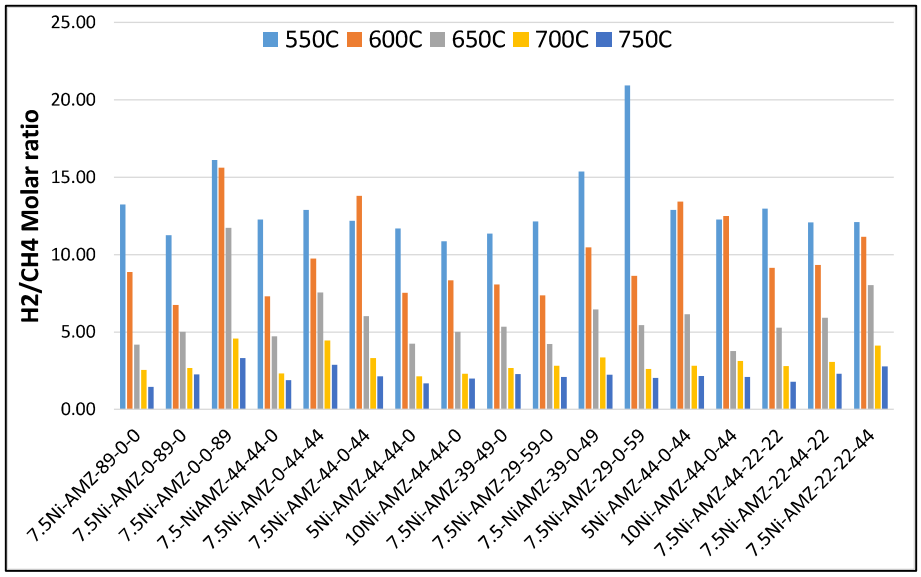

Figure 111: Trend of H_2/CH_4 molar ratio at various temperatures for various catalysts

The decrease in the ratio of H_2/CH_4 can be attributed to the formation of methane in-situ due to side reactions such as methanation of CO or the catalytic decomposition of ethanol.

A comparison of trends of H_2/CO, H_2/CH_4 and $XEtOH/XCO_2$ with reaction temperature is made below to throw light on the reactions taking place on the catalysts with different compositions and thus explain the difference in trends between them.

Comparing the trend of yields of H_2, CO, CH_4, conversion of EtOH and conversion of CO_2 and the above-mentioned ratios with increasing reaction temperature, it is observed that:

1. Both H_2/CO (Figure 110) and XEtOH/XCO_2 (Figure 109) increase with reaction temperature. However, the trend of H_2/CO with temperature differs with the catalyst composition. Catalysts that contain Zr (AMZ-0-0-89, AMZ-44-0-44, AMZ-39-0-49 or AMZ-29-0-59) show an increase in the ratio H_2/CO over the entire temperature range studied (550°C-750°C) whereas binary and ternary catalysts containing Mg show a plateau at the higher temperature. The former shows a decrease in the yield of CO whereas the latter does not show a significant change in yield of CO with temperature. Based on the stoichiometric trends shown in Table 8 this trend in the ratio of Zr containing binary and ternary catalysts can be explained by the WGS reaction: $CO + H_2O = H_2 + CO_2$ because it produces H_2 and CO_2. The H_2O is available from the dehydration of ethanol to ethylene and water. The consumption of CO with the attendant formation of H_2 increases the H_2/CO ratio whereas the formation of CO_2 increases the concentration of CO_2 in the product which manifests as a decrease in its conversion, thus, increasing the XEtOH/XCO_2 ratio. The other possibility is the disproportionation of CO (Boudouard reaction) $2CO = CO_2 + C$. This too increases both H_2/CO (because of the consumption of CO) and XEtOH/XCO_2 (due to the production of CO_2). However, it does not produce H_2. Figure 107 shows no significant change in the yield of H_2 with temperature for Zr-containing catalysts, whereas the yield of CO decreases (Figure 110). Thus, the relatively large change in H_2/CO of catalysts containing Zr (Figure 110) along with a higher amount of coke laydown on Zr-based catalysts (Figure 115) indicates that the Boudouard reaction (which consumes 2 moles of CO without producing H_2) is more probable between the two reactions in catalysts containing Zr. The H_2/CH_4 ratio (Figure 111) decreases sharply with increasing temperature for all catalysts. Figure 114 shows a sharp increase in yield of methane with reaction temperature. Catalyst deactivation is also markedly less. Thus, a possibility is the hydrogenation of coke (methanation) occurring concurrently with the WGS reaction. The methanation of CO under H_2 rich conditions: $CO + 3H_2 = CH_4 + H_2O$ or under H_2 lean conditions: $2H_2 + 2\ CO =$

CH_4 + CO_2 (more probable) can also explain methane formation and the resultant decrease in H_2/CH_4 ratio. However, neither reaction can explain the increase in H_2/CO with reaction temperature which is observed for these catalysts. Thus, the trend can be explained only if the methanation reaction (most probably $2H_2+2CO = CH_4+CO_2$, which produces methane) is occurring concurrently with the Boudouard reaction (which consumes 2 moles of CO without consuming or producing H_2) or the WGS which forms H_2. One mole of H_2 is formed per mole CO in the WGS reaction whereas 2-3 moles of H_2 are consumed in methanation. which can explain a decrease in H_2/CH_4 ratio. WGS is a reversible reaction which is not favored at high reaction temperatures. The exact mechanism could not be pinpointed.

2. On the other hand, in the case of catalysts that contain Mg (AMZ-0-89-0, AMZ-44-44-0, AMZ-39-49-0, AMZ-29-59-0) the yield of H_2 shows an overall increase with some anomalies with increasing temperature. The yield of CO also shows an overall decrease with increasing temperature with anomalies. The overall effect is an increase in the ratio of H_2/CO up to 650°C followed by a plateau at higher temperatures, which is different from that of the Zr containing binary and ternary catalysts where this ratio increases with reaction temperature. The ratio of H_2/CH_4 decreases significantly with temperature for all catalysts indicating the formation of methane. The trend of the yield of methane (Figure 114) corroborates this observation. The ratio $XEtOH/XCO_2$ increases with increasing reaction temperature. The plateau behavior of H_2/CO in binary and ternary catalysts containing Mg can be explained by the methanation reaction occurring under lean H_2 conditions: $2H_2 + 2\ CO = CH_4 + CO_2$. Since equimolar CO and H_2 react, their ratio remains unchanged which explains the plateau in H_2/CO. One mole of methane is formed for every 2 moles of H_2 which decreases the H_2/CH_4 ratio sharply. And the CO_2 formed increases its concentration in the reaction product which manifests as a decrease in the conversion of CO_2, which in turn increases the XEtOH/XCO= ratio. The mechanism below reaction temperature 650°C appears to be the same as for the zirconia-containing catalysts.

5.5: By-Products

The trend of the yield of ethylene is shown in Figure 112 below.

As seen from this Figure the trend is mostly linear with temperature. The trend of the yield of ethylene for binary catalysts is Al>Zr>>Mg. The binary Mg catalyst shows a significantly lower yield than the Al or Zr catalysts. Bellido et.al [10] have reported similar trend with increase in the yield of ethylene with an increase in temperature from 600°C to 800°C for dry reforming of ethanol on Ni/Y_2O_3-ZrO_2 catalysts wherein the Ni is added by impregnation.

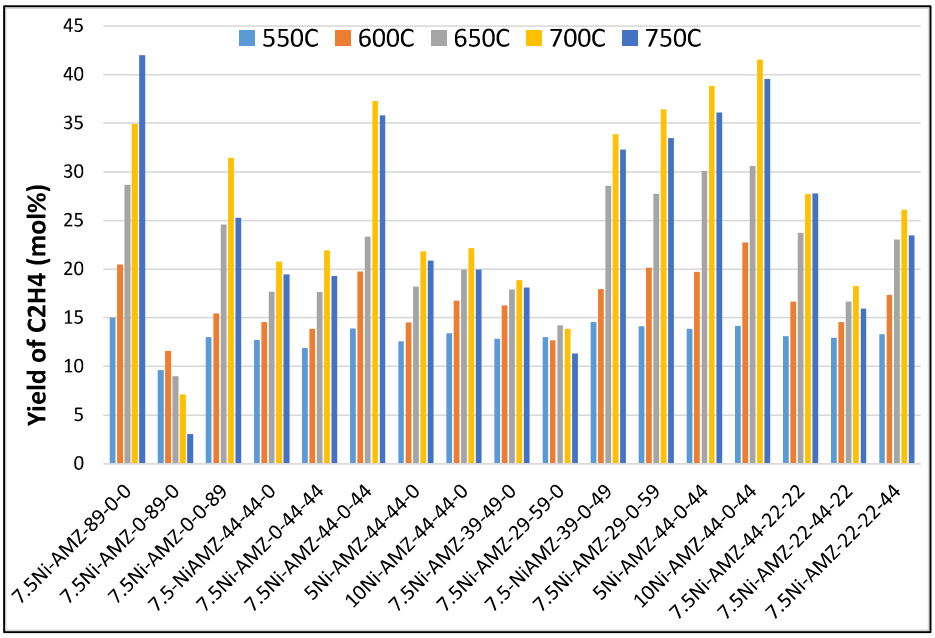

Figure 112: Trend of Yield of Ethylene at various temperatures for various catalysts

For ternary catalysts, the trend is balanced Al-Zr≥skewed Al-Zr>balanced Al-Mg>skewed Al-Mg. The Al-Mg catalysts show significantly lower yield than Al-Zr catalysts. For quaternary catalysts, the trend is Al-rich>Zr-rich>Mg-rich. There is no significant trend of the yield of C_2H_4 with Ni content of the catalyst for both AMZ-44-0-44 and AMZ-44-44-0 series.

Between the series, the trend is binary Al>balanced Al-Zr>skewed Al-Zr>binary Zr=quaternary Al-rich>quaternary Zr-rich>balanced Al-Mg=Mg-Zr>skewed Al-Mg>Binary Mg

As regards the trend with temperature, the binary Mg catalyst shows a clear decrease in the yield of C_2H_4 with increasing temperature and the ternary skewed Al-

Mg catalysts show a maximum (hyperbolic) or flat trend. The binary Al or Zr and ternary Al-Zr and all the quaternary catalysts show an increase.

The trend of yield of ethylene at 550°C and 750°C is compared with the strong acidity of the catalysts in Figure 113 below:

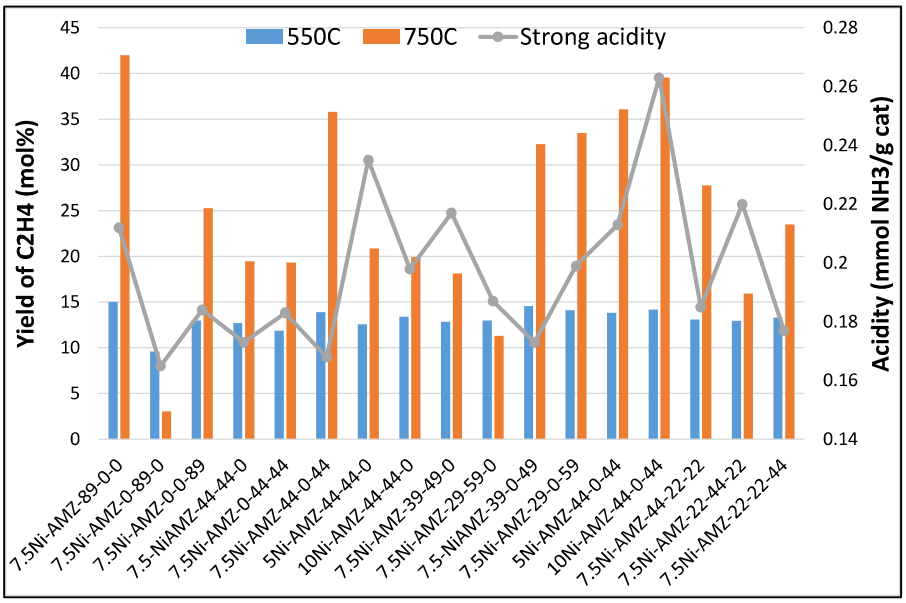

Figure 113: Trend of Yield of Ethylene at 550°C and 750°C with Strong acidity of various catalysts

As seen from the Figure, despite some anomalies, there is a fair trend between the yield of ethylene at 750°C and strong acidity of the catalyst. Incidentally, the Zr-based catalysts which show higher strong acidity also show more coke content for operation at 750°C (Figure 118). Thus, there appears to be a relation between coke and ethylene yield, both of which are influenced by acidity. Ethylene is known to laydown coke by its polymerization on acidic materials, as reviewed by Meng Ni et.al [22] for the reforming of bioethanol. Vizcaino A.J et.al [23] have prepared and studied layered double hydroxides (LDH) of Ni, Al and Mg by homogeneous alkalinization. Although they have not studied acidity, they report absence of ethylene in these catalysts. They also report significantly low coke formation compared to catalysts not containing Mg. They attribute this to neutralization of acid sites which mitigates formation of ethylene by dehydration. Aupretre F et.al. [24] have studied Mg-Ni-Alumina spinels and directly correlated decrease in ethylene selectivity with basicity of the catalyst as determined by CO_2 chemisorption and acidity determined by the isomerization of dimethyl-3,3-but-1-ene.

The trend of CH_4 of the catalysts is shown in Figure 114 below. As seen in the Figure below, the trend is exponential.

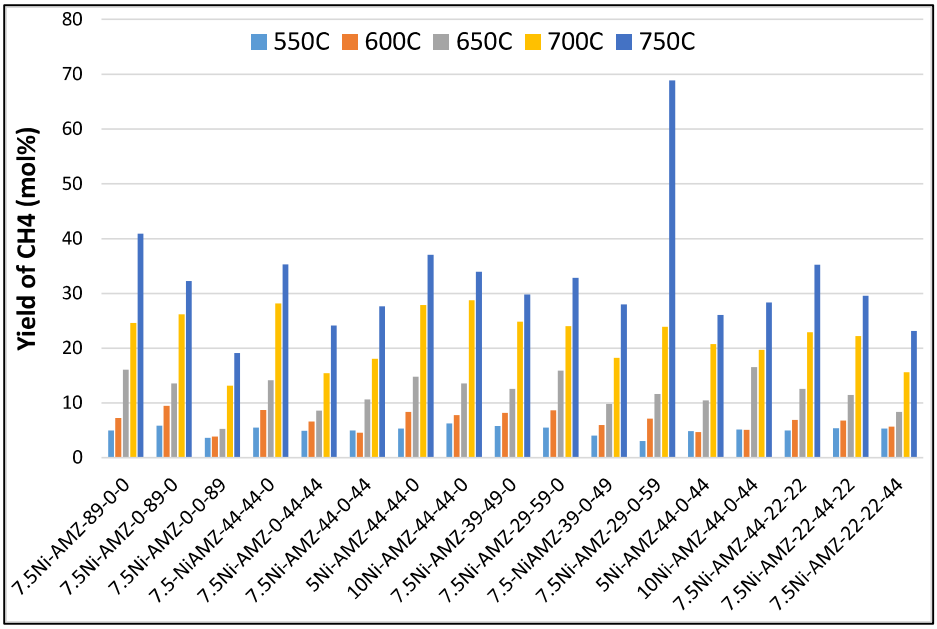

Figure 114: Trend of Yield of Methane at various temperatures for various catalysts

As seen from figure 114 above the yield of methane increases with increasing reaction temperature. Bahari et.al [8] who have studied dry reforming of ethanol on Ce promoted Ni/Al_2O_3 catalysts report a similar sharp increase with temperature in the range 647°C-697°C. Bellido et.al. [10] have also reported a similar trend for 5% Ni/Y_2O_3-ZrO_2 catalysts prepared by impregnation of Ni. They have varied temperature from 600°C to 800°C in their studies. They too observe a sharp increase when the temperature is increased from 600°C to 700°C.

As seen from Figure 114 above the trend for binary catalysts is Al>Mg>Zr. This is different from that of ESR, where it is Mg>Al>Zr. For the ternary catalysts, the trend is Al-Mg > Al-Zr > Mg-Zr. The yield of methane decreases with increasing Ni content for the AMZ-44-44-0 series whereas the AMZ-44-0-44 series do not show a clear trend. The trend for quaternary catalysts is Al rich>Mg rich >Zr rich which is again different from that of ESR.

Between the series, the trend is ternary balanced Al-Mg >Binary Al = binary Mg > Quaternary Al-rich>skewed Al-Mg>Quaternary Mg-rich> Al-Zr>ternary Mg-Zr≥Quaternary Zr-rich>Binary Zr.

As also observed in ESR methane yield increases significantly at ≥700°C.

5.6: Catalyst Stability- Screening studies

The effect of catalyst composition on the formation of coke is shown in Figure 115 below. The catalysts were operated at 750°C for 8 hours.

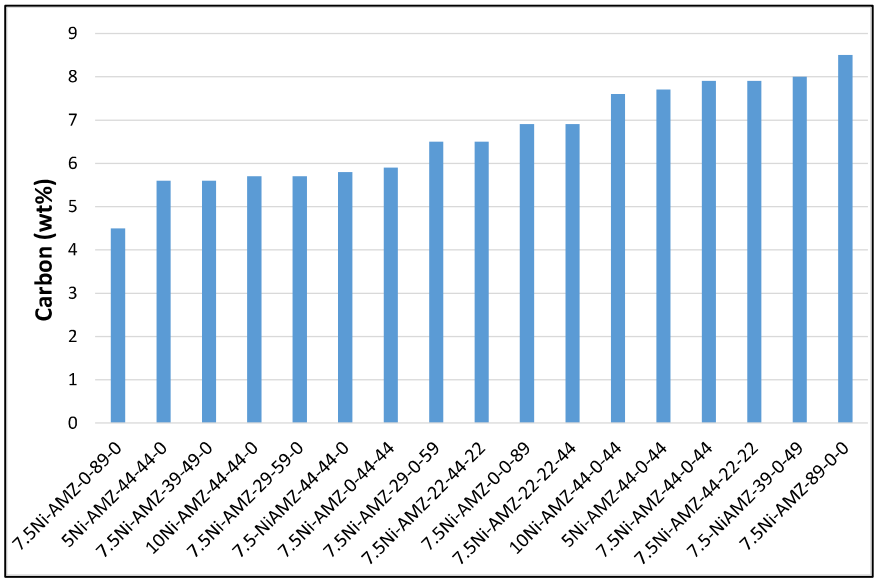

Figure 115: Coke formation of various catalysts operated at 750°C for 8 hours.

As seen in Figure 115, coke content of the catalyst determined by CHN analysis ranges from 4.5wt% to 8.5wt%. Bellido et.al [10] have reported coke 3.48 wt% - 4.8 wt% coke for spent Ni supported on Y_2O_3-ZrO_2 catalysts at 600°C. The coke content observed in the current study is higher. Bahari et.al [8] have characterized coke deposits on spent catalysts by Raman spectroscopy and determined that promotion of Ni/Al_2O_3 catalysts by Ce decreases the amorphous coke content from 71.8% to 67.6%. The rest being crystalline coke. They have not provided the quantity of coke deposited on the catalyst.

The trend for the binary catalyst is Al>Zr>>Mg. For ternary catalysts, the trend is Al-Zr >Mg-Zr>Al-Mg. No difference is observed between the balanced and skewed Al-Mg ternary catalysts. Similarly, no difference was observed between balanced and skewed Al-Zr ternary catalysts for Zr/Al weight ratio 1.256 (AMZ-39-0-49). Increasing this ratio to 2.03 (AMZ-29-0-59) results in a significant decrease in Coke content from about 8.0 wt% to 6.5 wt%. OSC (oxygen storage capacity) measurements reported in Chapter 2 section 2.3.5 clearly show the influence of Zr on OSC. Thus, it appears that increasing Zr content retards coke formation in ternary Al-Zr catalysts due to

scavenging of coke by mobile oxygen. However, this advantage was not observed in ESR, where the AMZ-29-0-59 catalyst showed the highest coke content among all the catalysts. Therefore, it appears the OSC plays a significant role in scavenging coke in EDR but not in ESR. The trend for quaternary catalysts is Al-rich>Zr-rich>Mg-rich. Thus, overall catalysts containing Zr show higher coke content (except AMZ-29-0-59).

Zr content was not varied for the ternary Mg-Zr catalysts. It is recommended to study this in future work.

Figure 116 below compares coke deposited on the catalyst in ESR with that in EDR for short duration runs (8 hours) at 750°C.

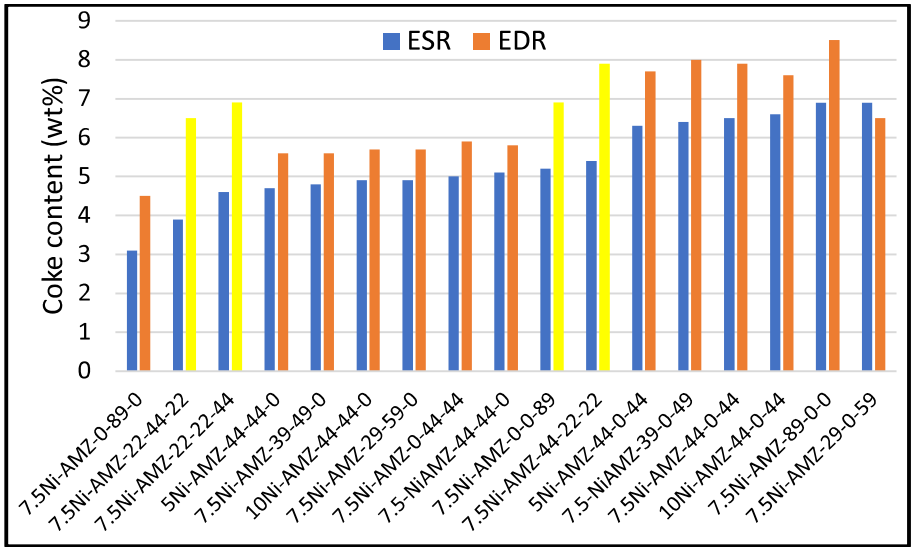

Figure 116: Comparison of coke content of spent catalysts used for short duration (8 hours) ESR and EDR runs.

As seen from this Figure all the catalysts show higher coke formation in EDR than in ESR. The overall trend with respect to catalyst composition is similar for both ESR and EDR (the ternary Al-Zr catalysts and the binary Al catalyst show higher coke content than the binary Mg or ternary Al-Mg catalysts). However, the binary Zr catalyst AMZ-0-0-89 and all three quaternary catalysts (bars shown in yellow color) show significantly more coke in EDR than in ESR. The Mg and Zr rich quaternary catalysts show higher coke content than ternary Al-Mg catalysts which is contrary to the trend observed in ESR. Similarly, the Al rich quaternary catalyst shows coke content like that of ternary Al-Zr catalysts (again unlike in ESR, where it showed less coke). Thus, it appears that the presence of Zr in addition to Mg in quaternary catalyst opposes

/obscures the beneficial effect of Mg which is otherwise seen in steam reforming of ethanol.

Coking rate calculated for the 8 hour runs range from 5.6 to 10.6 mg C/h/ g cat. As expected from the higher coke content of spent catalysts used for EDR, these rates are higher than those observed in ESR. Se-won Park et.al [25] have reported coke 1.2 mg/mg ethanol reacted. Based on their reaction conditions 0.5g catalyst, 40000 h^{-1} gas hourly space velocity, 5 vol% each of CO_2 and ethanol, balance He, this works out to 7.4 mg C/h/g cat which is close to the value of 8.5 mg C/h/g cat observed in the current study. Shulin Zhao et.al. [21] have reported values of 0.28 mg C/h/g cat for Rh/CeO_2 catalyst at 700^{o}C and CO_2/ethanol 3. Which is in line with most reports which state that noble metal catalyst form significantly less coke, besides the choice of reaction conditions.

The trend of coke content is compared with the strong acidity of the catalysts in Figure 117 below.

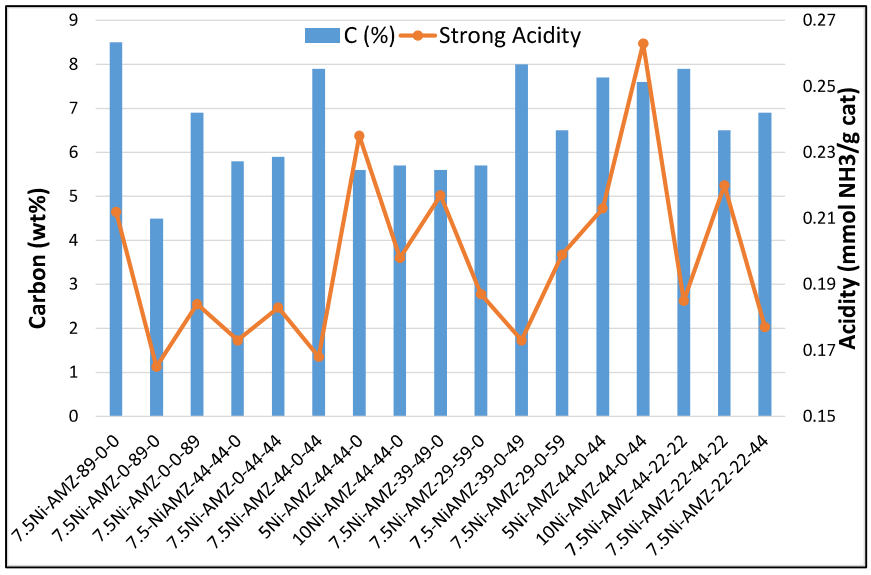

Figure 117: Trend of Coke content and Strong acidity for various catalyst

As seen from this Figure, there is a qualitative trend, but the correlation is not strong. Thus, it appears that the polymerization of ethylene, which is an acid-catalyzed reaction, is not the only contributor to coke. Other reactions such as the disproportionation of CO and methane also appear to contribute to coke formation.

The trend of decay constants (slope of decrease in conversion with time on stream) at 550°C and 750°C for a short duration (8 hours) runs is shown in Figure 118 below.

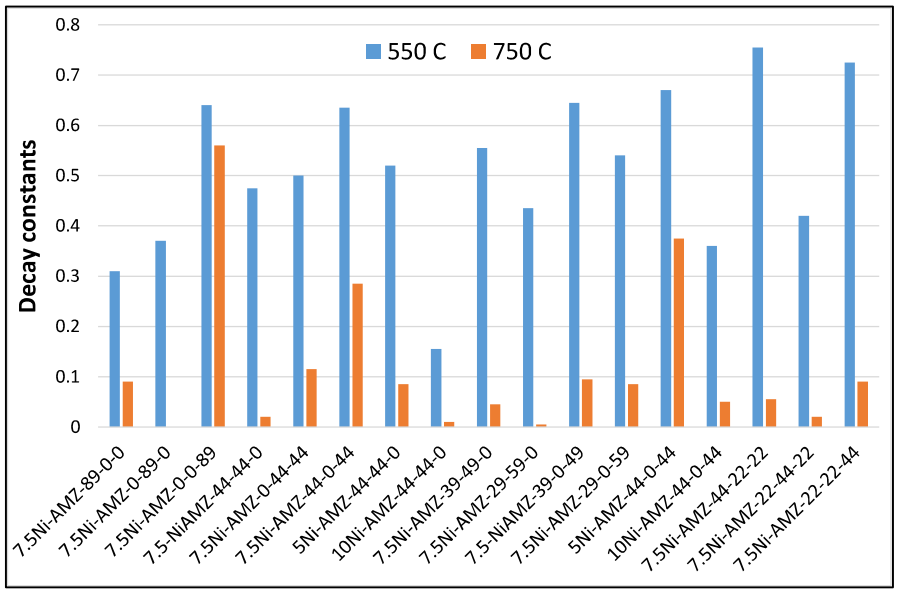

Figure 118: Trend of decay constants at 550°C and 750°C for 8 hours runs at various temperature for various catalysts.

As seen from the above Figure the trend based on composition for runs at 550°C is Al<Mg<Zr for the binary catalysts. Amongst the ternary catalysts except for AMZ-29-59-0 (which shows a smaller value), the remaining catalysts with 7.5% Ni content show similar decay constants. AMZ-39-0-49 and AMZ-44-0-44 show the highest decay constants. Decay constants decreases with increasing Ni content for both the AMZ-44-0-44 and AMZ-44-44-0 series. Between the two series, the ternary Al-Mg show smaller decay constants than the Al-Zr series. The trend for quaternary catalysts is Mg-rich<Zr-rich<Al-rich. Thus, the contribution of Magnesia to slow deactivation is not observed for binary catalysts at 550°C.

At 750°C there is a sharp drop in the magnitude of decay constants for most of the catalysts. Binary zirconia (AMZ-0-0-89) is the only catalyst that does not show this trend. At 750°C the trend for binary catalysts changes to Mg<<Al<<Zr. For ternary catalysts with 7.5% Ni content, the trend is AMZ-29-59-0< AMZ-44-44-0< AMZ-39-49-0< AMZ-29-0-59< AMZ-39-0-49< AMZ-0-44-44> AMZ-44-0-44. Hence, skewed, and balanced Al-Mg catalysts show the slowest deactivation (highest stability). Both the AMZ-44-0-44 and AMZ-44-44-0 series show a trend of decreasing magnitude of

the decay constant with increasing Ni content. The catalysts with 10wt% Ni show smaller decay constants in both the AMZ-44-44-0 and AMZ-44-0-44 series. Amongst the quaternary catalysts, the trend is Mg-rich<Al-rich<Zr rich. Thus, catalysts containing Mg irrespective of whether they are binary, ternary, or quaternary, show slower deactivation at 750°C. The binary Mg catalyst shows the slowest decay constant followed by ternary AMZ-29-59-0 amongst all the catalysts. The ternary Al_2O_3-ZrO_2 and binary ZrO_2 support which show the highest OSC (oxygen storage capacity), show faster deactivation than the ternary Al_2O_3-MgO and binary magnesia catalysts. However, within the Al-Zr series, decay constants decrease with increasing zirconia content of the support. Thus, OSC does appear to influence deactivation. Interestingly the quaternary Mg-rich catalyst shows slow deactivation comparable with even the ternary Al-Mg catalyst with a balanced composition. Whereas the quaternary catalyst which is rich in Zirconia shows faster deactivation. The binary Zirconia catalyst shows the fastest deactivation among all the catalysts.

In studies of Rh/CeO_2 catalysts for dry reforming of ethanol carried out by Shulin Zhao et.al. [21], the authors have observed a decrease in coke formation when partial pressure of CO_2 is increased in the feed. They also report CO_2 conversion higher than stoichiometric for dry reforming of ethanol and attendant increase in concentration of CO in the product. They attribute this to the reverse Boudouard reaction: $CO_2 + C = 2CO$

The trend of product distribution with reaction temperature is very different in the current study. Conversion of CO_2 decreases indicating an increase in its concentration in the product. Concentration of CO also decreases whereas methane increases significantly with increasing reaction temperature. This suggests that hydrogenation of coke, $C + 2H_2 = CH_4$, may be occurring concurrently with WGS (which consumes CO and produces H_2 and CO_2) at the higher temperatures.

The relation between the magnitude of the decay constant and the coke content of spent catalysts operated at 750°C for 8 hours on stream is shown in Figure 119 below.

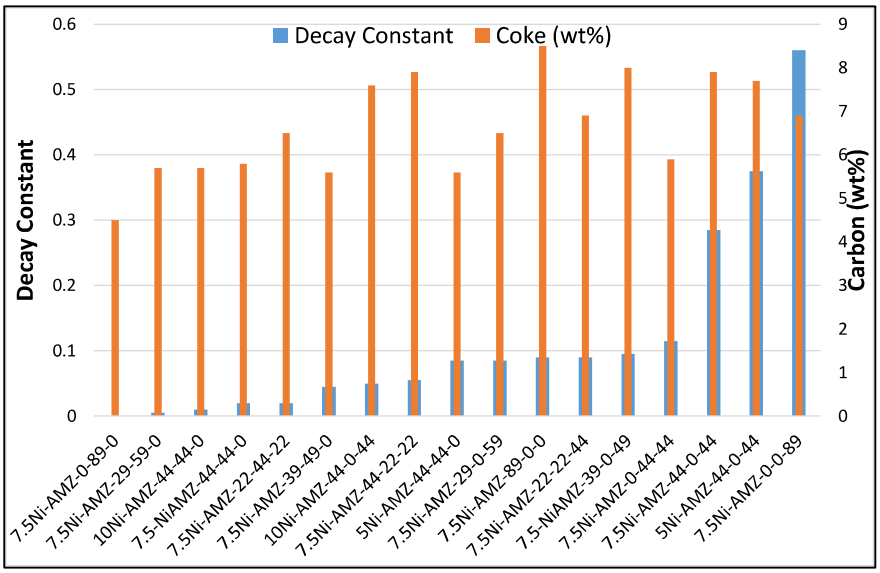

Figure 119: Trend of relation between the magnitude of the decay constant and the coke content of spent catalysts operated at 750°C for 8 hours.

As seen from this Figure the coke content varies between 4.5 wt% to 8.5 wt%. Catalysts containing magnesia show smaller decay constants as well as lower coke content than catalysts containing zirconia. The binary alumina catalyst presents the highest content of coke with a relatively small decay constant, whereas the binary Zr catalyst presents the highest decay constant with significant coke formation. The Al-Zr ternary catalysts with balanced composition also show high coke content with large decay constants. The remaining catalysts show significantly smaller decay constants. The binary magnesia catalyst shows the lowest Coke content as well as the smallest decay constant across all the catalysts. Thus, unlike ESR there is no correlation between coke content and value of decay constant. Coke content is disproportionately large compared to the magnitude of the decay constant. Which indicates that the binary Mg, ternary Al-Mg, ternary skewed Al-Zr and quaternary catalysts have a high capacity for accommodating coke.

Linear regression analysis of coke deposited versus decay constant shows a poor relationship between the two with a correlation constant (R^2) of 0.17. Sintering of Ni is observed for 7.5%Ni-AMZ-44-0-44 where particle size of Ni(0) increases by 66.3% and for 7.5%Ni-AMZ-22-44-22, where the increase is 67%. These catalysts did not show such a large increase in particle size in ESR. Thus, both coke deposition and active metal sintering result in a drop in conversion (deactivation).

5.7: Long-duration run (80 hours)

Catalyst 7.5%Ni-AMZ-44-0-44 (ternary balanced Al-Zr) and quaternary 7.5%Ni-AMZ-22-44-22 were subjected to long-duration runs at 80 hours each at 650°C and 700°C. The basis for their selection was that AMZ-0-89-0 which showed very slow deactivation in short-duration runs in ESR showed fast deactivation in long-duration runs. 7.5%Ni-AMZ-44-0-44 and 7.5%Ni-AMZ-22-44-22 showed high and low deactivation respectively in short-duration runs for EDR. Between these 7.5%Ni-AMZ-22-44-22 showed the slowest deactivation amongst the series and it is a quaternary catalyst that contains all three elements Al, Mg and Zr.

The results of time on stream conversion of EtOH for catalysts 7.5%Ni-AMZ-44-0-44 are shown in Figure 120 below.

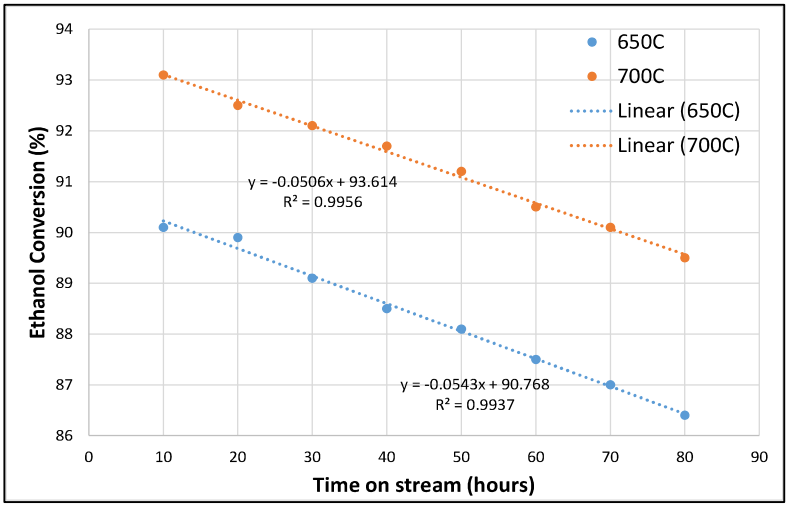

Figure 120: Ethanol Conversion for 7.5%Ni-AMZ-44-0-44 Catalyst at 650°C and 700°C.

As seen from this Figure conversion of ethanol is higher at 700°C. Conversion decreases with time on stream for both catalysts. The slope of decay in conversion with time is slightly lower for the run at 700°C. The trend is like that observed for the short (8 hours duration runs – Figure 119 above), wherein deactivation slows down with increasing reaction temperature. Further, the decay slope is significantly smaller than for the short duration runs. This trend is like what was observed in ESR.

The trend of conversion of CO_2 of catalyst 7.5%Ni-AMZ-44-0-44 with time on stream for the 80 hours run is shown in Figure 121.

As seen from the Figure the conversion is lower at 700°C than at 650°C. The trend is like that obtained in the short duration runs.

The average H_2/CO ratio was 3.08 at 650°C and 3.35 at 700°C which are in the ballpark range of the short duration runs where the values were 2.72 and 3.23 respectively.

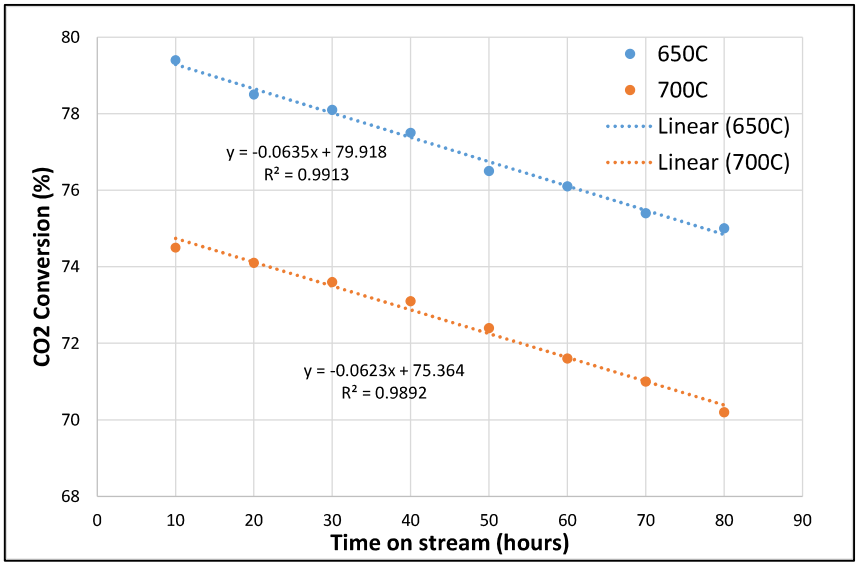

Figure 121: CO_2 Conversion for 7.5%Ni-AMZ-44-0-44 Catalyst at 650°C and 700°C

The fresh reduced and stabilized catalyst shows median Ni particle size 10.7 nm with a range 8 to 25.7 nm, whereas the spent catalyst after EDR showed median particle size 17.8 nm (66.3% increase) with range 12 to 36 nm.

The trend of conversion of ethanol with time on stream for catalyst 7.5%Ni-AMZ-22-44-22 is shown in Figure 122 below.

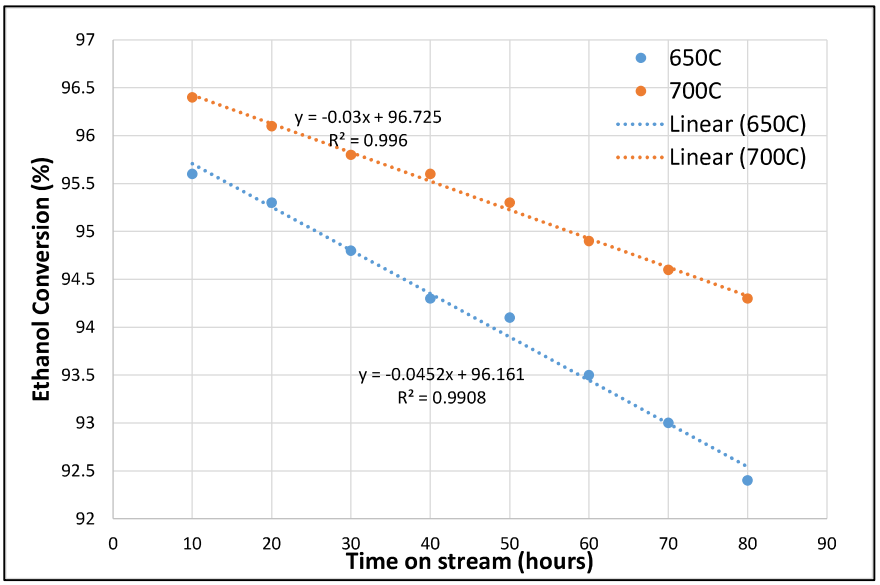

Figure 122: Ethanol Conversion for 7.5%Ni-AMZ-22-44-22 Catalyst at 650°C and 700°C.

As seen from this Figure, the trend is like that of catalyst 7.5%Ni-AMZ-44-0-44 and the short duration run of 7.5%Ni-AMZ-22-44-22. The 7.5%Ni-AMZ-22-44-22 catalyst shows slower deactivation than 7.5%Ni-AMZ-44-0-44 which is also consistent with the trend of short duration runs (Figure 120 above). Deactivation is also slower at the higher temperature.

The trend of conversion of CO_2 of 7.5%Ni-AMZ-22-44-44 is shown in Figure 123 below.

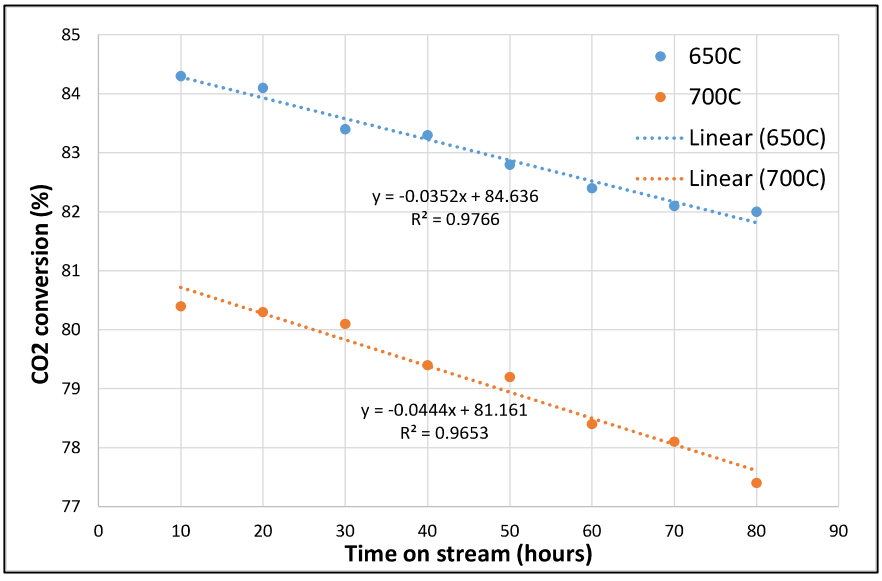

Figure 123: CO_2 Conversion for 7.5%Ni-AMZ-22-44-22 Catalyst at 650°C and 700°C

As seen from Figure 123, the trend is like that of AMZ-44-0-44 (Figure 121) above, however decay constants are smaller.

The average H_2/CO values at 650°C and 700°C are 2.34 and 2.77 respectively. These are in the ballpark range of values for the short duration runs which are 2.31 and 2.55 respectively.

The fresh reduced and stabilized catalyst shows median Ni particle size 13.3 nm with a range 8.8 nm to 17.7 nm, whereas the spent catalyst after EDR shows median particle size 22.2 nm (67% increase) with range 17 nm to 52.3 nm.

Thus, Ni metal sintering is observed in EDR even for catalysts which do not present it in ESR.

5.8: Coke Morphology by HRTEM

The morphology of coke deposited on catalysts 7.5%Ni-AMZ-44-0-44 and 7.5%Ni-AMZ-22-44-22 in long duration runs 80 hours each at 650°C and 700°C, LHSV 8h-1 (on ethanol), pressure atmospheric, EtOH: CO_2 1 molar, Nitrogen: EtOH molar ratio 1.0 was determined by HRTEM. Refer Figure 124.

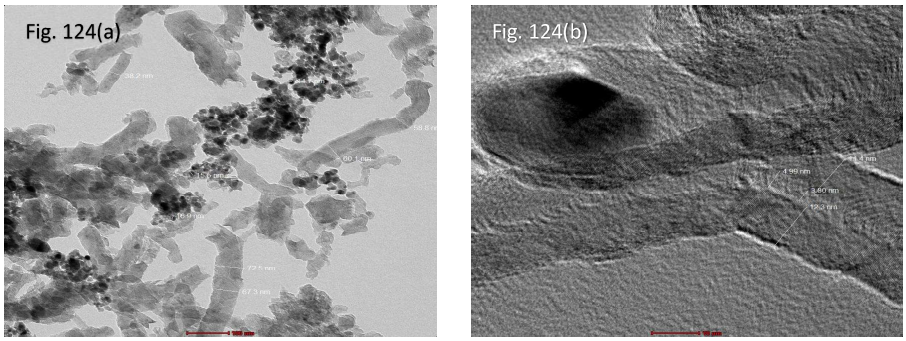

Figure 124: HRTEM micrograph of catalyst 7.5%Ni-AMZ-44-0-44

As seen from Figure 124 the morphology of coke is hollow filamentous/whisker type. The hollow nature of filamentous/whisker carbon has been reported earlier by S Helveg et.al [26]. They quote Baker et.al. [27] who have proposed the hollow nature even earlier. The presence of Ni particles at the end of the filaments suggests a tip growth mechanism (refer Figure 124 (b)). This is different from the morphology of coke observed for this catalyst in ESR. In ESR the coke was rod-like and showed base growth. Bahari et.al [8] have reported whisker type coke on Ce-promoted Ni/Al_2O_3 catalysts for dry reforming of ethanol. Fayaz et.al [6] have also reported filamentous

carbon in dry reforming of ethanol on La promoted Co/Al_2O_3. Both Bahari and Fayaz report formation of encapsulating coke on the un-promoted catalysts. The Ni/Al_2O_3 binary catalyst was not characterized by HRTEM is the current study.

The figure on the left shows a ridge running along the central axis of the filament. This type of filament is reported to form when the growth of the same filament takes place on two adjacent facets of the metal particle. The entrance to the filament is also seen which appears to have a pear-shaped nickel particle within it at the tip (Figure 124 (b)). The coke content of the spent catalyst was 13.4% and this catalyst presented a decay slope of 0.0506.

The HRTEM of the spent catalyst 7.5%Ni-AMZ-22-44-22 is shown in Figure 125 below.

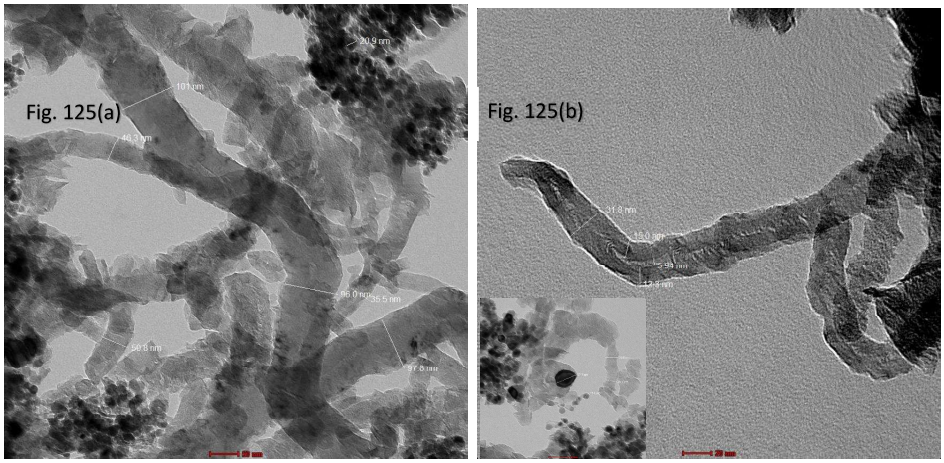

Figure 125: HRTEM of the spent catalyst 7.5%Ni-AMZ-22-44-22

As seen from this Figure the morphology of coke is again filamentous. The presence of Ni particles at the tip of the filament indicates tip growth (inset of Figure 125 (b)). Small particles of Ni are observed at different locations within the carbon filaments, like what is reported by Helveg et.al [26]. Like 7.5%Ni-AMZ-44-0-44, this catalyst also showed a different morphology viz. whisker carbon with a broad base and tapering tip in ESR studies. The coke content of this catalyst was 12.3% and the decay

slope was 0.03. Based on limited results it appears that coke morphology is not sensitive to catalyst composition in EDR which is very different from that of ESR.

5.9: Catalyst Regeneration

Catalyst 7.5%Ni-AMZ-22-44-22 was tested for its regenerability. The spent catalyst from the 80 hours run was regenerated by controlled oxidation at 550°C and 650°C. The comparison of ethanol conversion for the fresh catalyst and the regenerated catalyst is made in Figure 126 below.

When the spent catalyst is regenerated at 550°C initial catalyst activity is not only lower (by 5.8 units), but rate of decay of conversion is also very steep (slope 0.431) than that of the fresh catalyst (0.054). When the same spent catalyst is regenerated at 650°C initial activity improves (3.6 units lower than fresh catalyst) and the slope of decay of conversion is comparable to that of the fresh catalyst (0.052 versus 0.054). The loss in initial activity indicates some irreversible deactivation. As highlighted in sections above the spent catalyst shows 12.3% coke and a 67% increase in particle size of Ni(0).

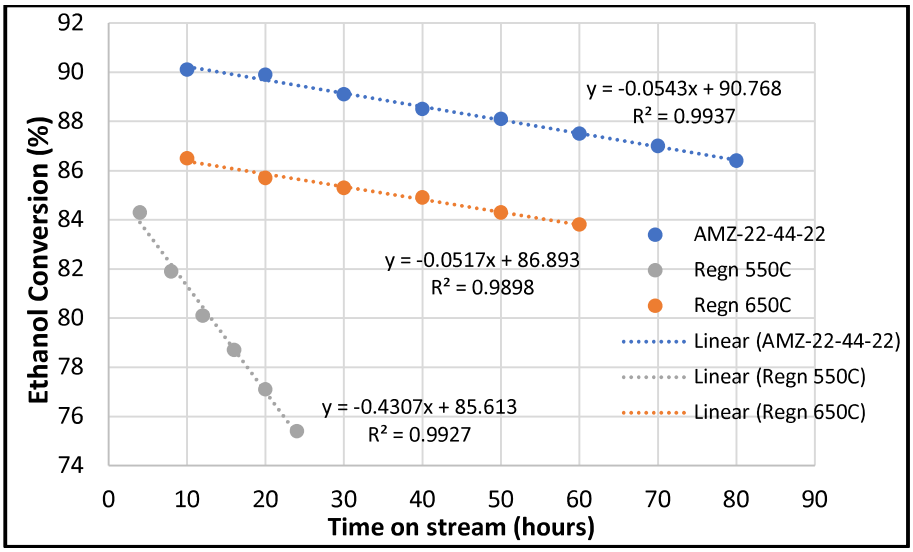

Figure 126: Ethanol conversion for the fresh and regenerated 7.5%Ni-AMZ-22-44-22 catalyst

From this, it is clear that the coke is refractory in nature and 550°C is insufficient for its complete combustion, which results not only in lower initial activity but also faster deactivation of the catalyst. When the catalyst is regenerated at 650°C this coke combusts completely. Initial activity improves but it is still lower than that of the fresh

catalyst due to the significant sintering of Ni metal during use for EDR. Bahari et.al [8] have quantified amorphous and graphitic coke deposited on Ce-promoted Ni/Al_2O_3 catalyst using Raman spectroscopy. They report that the former is in a larger proportion than the latter (ratio of amorphous to graphitic 2.05-2.55). Fayaz et.al. [6] have carried out TPO studies of carbon deposited on La-doped Co/Al_2O_3 catalysts. They attribute the refractory high temperature combustion peak (527^oC-627^oC) to graphitic coke.

5.10: Conclusions

The dry reforming of ethanol is a reaction that has the double advantage of decreasing the carbon footprint. It not only uses a reactant that is renewable but also consumes and valorizes CO_2 by utilizing it as a co-reactant.

Like steam reforming, dry reforming consists of many reactions which are thermodynamically feasible and lead to similar products viz. H_2, CO, CH_4, C_2H_4 and carbon.

The same set of 17 catalysts that were used in the steam reforming of ethanol was used for the dry reforming.

Correlation of catalyst activity such as composition, BET-specific surface area, acidity, metal dispersion and OSC with catalyst activity (in terms of ethanol conversion) are like those observed for ESR.

The results indicate that Mg-based catalysts show higher conversion of ethanol. While the conversion of ethanol increases with reaction temperature, the conversion of CO_2 decreases indicating a change in the reaction mechanism with increasing temperature.

The correlation of ratios of H_2/CO, H_2/CH_4 and conversion of ethanol/conversion of CO_2 is utilized to understand the reaction mechanism of the catalyst composition. Catalysts that contain Mg show distinct differences from those which do not contain Mg. Catalysts containing Zr appear to promote the Boudouard reaction rather than the WGS reaction or WGS concurrently with methanation. The trend of H_2/CH_4 is explained by the methanation of CO at lean H_2 conditions occurring concurrently with the Boudouard reaction or with WGS.

Whereas in catalysts which contain Mg the trends at ≥650°C are explained by the methanation of CO at hydrogen lean conditions those at temperature <650°C the Boudouard reaction occurs concurrently with the methanation reaction like catalysts which contain Zr.

Binary and ternary catalysts which do not contain Mg show a significantly higher yield of ethylene and this correlates reasonably well with the acidity of the catalysts. The dehydration of ethylene is an acid-catalyzed reaction. Hence the trend conforms to expectations.

As seen from this study the product distribution is influenced significantly by inherent chemical activity (which is dependent on the composition of the catalyst).

Coke deposition also trends well with composition and acidity. Catalysts with higher acidity form more coke.

Like ESR two regimes viz. a faster short-term and a slower long-term deactivation are observed. Trends of decay of ethanol conversion with composition are markedly different for low temperature (550°C) and high temperature (750°C) which indicate that different reactions take place at these temperatures. Further, the decay of ethanol conversion is significantly slower at higher temperatures than at lower temperatures which is like in ESR. Methanation of coke by H_2 to form CH_4 is consistent with the trend of yield of methane with reaction temperature.

OSC influences deactivation. Increasing the zirconia content of support (which increases OSC in turn) slows down deactivation in ternary Al-Zr catalysts. Decay of ethanol conversion does not show a good correlation with coke content indicating that coking is not the only cause for catalyst deactivation. Sintering of Ni is observed in ternary Al-Zr and quaternary Mg rich catalysts which do not show this behavior in ESR.

Long-duration runs present slower deactivation which is like that observed in ESR. The Coke morphology of 7.5%Ni-AMZ-44-0-44 and 7.5%Ni-AMZ-22-44-22 which present slow deactivation in long duration runs is filamentous. It is significantly different from that formed in ESR where it was either rod-like or whisker/tentacle with a broad base and tapered tip.

Both ternary Al-Zr catalyst 7.5%Ni-AMZ-44-0-44 and quaternary catalyst 7.5%Ni-AMZ-22-44-22 present irreversible deactivation due to sintering of Ni(0)

during use for EDR. The coke on the spent catalysts is refractory and requires higher temperature for combustion.

Thus, catalyst composition and the interaction between individual components of the catalyst play a significant role in governing activity, product selectivity and catalyst stability. Cause of deactivation is different from that EDR.

References:

1) Jie Yu, José A. Odriozola, Tomas R. Reina, Dry reforming of ethanol and glycerol: Mini review; Catalysts; 9(12) (2019); 1015
2) Tormena M.M. and Pontes R.M.; A DFT/EDA study of ethanol decomposition over Pt, Cu and Rh metal clusters; Molecular Catalysis; 482(10) (2019); 110694.
3) Asmaa Drifa, Nicolas Biona, Rachid Brahmib, Satu Ojalac, Laurence Pirault-Roya,Esa Turpeinenc, Prem Kumar Seelamc, Riitta L. Keiskic, Florence Eprona; Study of the dry reforming of methane and ethanol using Rh catalysts supported on doped alumina; Applied Catalysis A: General; 504 (2015); 576–584.
4) A. Zawadzki, J.D.A. Bellido, A.F. Lucrédio, E.M. Assaf; Dry reforming of ethanol over supported Ni catalysts prepared by impregnation with methanolic solution. Fuel Processing Technology; 128 (2014); 432-440
5) Mahadi B. Bahari, Nguyen Huu Huy Phuc, Feraih Alenazey, Khanh B. Vu, Nurul Ainirazali Dai-Viet N. Vo; Catalytic performance of La-Ni/Al_2O_3 catalyst for CO_2 reforming of ethanol; Catalysis Today; 291 (2017); 67-75.
6) Fahim Fayaz, Long Giang Bach, Mahadi B. Bahari, Trinh Duy Nguyen, Khanh B. Vu, Ramesh Kanthasamy, Chanatip Samart, Chinh Nguyen-Huy, Dai-Viet N. Vo; Stability evaluation of ethanol dry reforming on Lanthana-doped cobalt-based catalyst for hydrogen rich syngas generation; International Journal of Energy Research; 43 (2019); 405-416.
7) Fahim Fayaz, Huong T. Danh, Chinh Nguyen-Huy, Khanh B. Vu, Bawadi Abdullah, Dai-Viet N. Vo; Promotional effect of Ce-dopant on Al_2O_3 supported Co catalysts for syngas production via CO_2 reforming of ethanol; Procedia Engineering; 148 (2016); 646-653.

8) Mahadi B. Bahari, Nguyen Huu Huy Phuc, Bawadi Abdullah, Feraih Alenazey, Dai-Viet N. Vo; Ethanol dry reforming for syngas production over Ce-promoted Ni/Al_2O_3 catalyst; Journal of Environmental Chemical Engineering; 4 (2015); 4930-4938.
9) Barnali Bej, Sujoy Bepari, Narayan C. Pradhan, Swati Neogi; Production of hydrogen by dry reforming of ethanol over alumina supported nano-NiO/SiO_2 catalyst; Catalysis Today; 291 (2017); 58-66.
10) Jorge D.A. Bellido, Eurico Y. Tanabe, Elisabete M. Assaf; Carbon dioxide reforming of ethanol over Ni/Y_2O_3-ZrO_2 catalysts; Applied Catalysis B: Environmental; 90 (2009); 485-488.
11) Mahadi B. Bahari, Nguyen Huu Huy Phuc, Bawadi Abdullah, Feraih Alenazey, Dai-Viet N. Vo; Ethanol dry reforming for syngas production over Ce-promoted Ni/Al_2O_3 catalyst; Journal of Environmental Chemical Engineering; 4 (2016); 4830-4838.
12) Tan Ji Siang, Mohd-Nasir Nor Shafiqah, Ponnusamy Senthil Kumar, Zainal Ahmad, A. A. Jalil, Mahadi B. Bahari, Quyet Van Le, Leilei Xiao, M. Mofijur, Changlei Xia, Shams Forruque Ahmed, Dai-Viet N. Vo; Advanced catalysts and effect of operating parameters in ethanol dry reforming for hydrogen generation: A review; Environmental Chemistry Letters; 20 (2022); 1695–1718.
13) Dong Cao, Fanli Zeng, Zijiao Zhao, Weijie Cai, Yi Li, Hao Yu, Shaoyin Zhang, Fengzuo Qu; Cu based catalysts for syngas production from ethanol dry reforming: Effect of oxide support; Fuel 219 (2018); 406-416.
14) Weijie Cai, Jiale Dong, Qing Chen, Tongkuan Xu, Shangru Zhai, Xianyun Liu, Li Cui, Shaoyin Zhang; One-pot microwave-assisted synthesis of Cu-$Ce_{0.8}Zr_{0.2}O_2$ with flower-like morphology: Enhanced stability for ethanol dry reforming; Advanced Powder Technology; 31 (2020); 3874-3881.
15) Xun Hu, Gongxuan Lu; Syngas production by CO_2 reforming of ethanol over Ni/Al_2O_3; Catalysis Communication; 10 (2009);1633-1637.
16) Hanfei Zhang, Ligang Wang, Jan Van herle, François Maréchal, Umberto Desideri; Techno-economic comparison of green ammonia production processes, Applied Energy; 259 (2020); 114135.
17) https://www.engineering.linde.com/dryref
18) https://www.chiyodacorp.com/en/service/gtl/co2-reforming/

19) Hongxue Zeng, Xinghong Qu, Dong Xu, Yang Luo; Porous adsorption materials for carbon dioxide capture in industrial flue gas.; Frontiers in Chemistry; 10 (2022).
20) Sepideh Jankhah, Nicolas Abatzoglou, François Gitzhofer; Thermal and catalytic dry reforming and cracking of ethanol for hydrogen and carbon nanofilament production; International Journal of Hydrogen Energy; 33; 4769-4779.
21) Shulin Zhao, Weijie Cai, Yi Li, Hao Yu, Shaoyin Zhang, Li Cui; Syngas production from ethanol dry reforming over Rh/CeO_2 catalyst; Journal of Saudi Chemical Society; 22 (2018); 58-65.
22) Meng Ni, Dennis Y.C. Leung, Michael K.H. Leung; A review on reforming bioethanol for hydrogen production; International Journal of Hydrogen Energy; 32 (15), (2007); 3238-3247.
23) A.J. Vizcaíno, P. Arena, G. Baronetti, A. Carrero, J.A. Calles, M.A. Laborde, N. Amadeo; Ethanol steam reforming on Ni/Al_2O_3 catalysts: effect of Mg addition; International Journal of Hydrogen Energy; 33(2008); 3489-3492.
24) Fabien Aupretre, Claude Descorme, Daniel Duprez, Dominique Casanave, Denis Uzio; Ethanol steam reforming over $Mg_xNi_{1-x}Al_2O_3$ spinel oxide-supported Rh catalysts; Journal of Catalysis; 233 (2005); 464-477.
25) Se-Won Park, Dongseok Lee, Seung-Ik Kim, Young Jin Kim, Ji Hoon Park, Iljeong Heo, Tae Sun Chang , Jin Hee Lee; Effect of alkali metals on Ni/alumina catalyzed ethanol dry reforming; Catalysts, 11 (2), (2021); 260.
26) S. Helveg, J. Sehested, J.R. Rostrup-Nielsen; Whisker carbon in perspective; Catalysis Today; 178 (2011); 42-46.
27) R.T.K. Baker, M.A. Barber, P.S. Harris, F.S. Feates, R.J. Waite; Nucleation and growth of carbon deposits from the nickel catalyzed decomposition of acetylene; Journal of Catalysis; 26(1) (1972); 51-62.

THIS PAGE IS LEFT BLANK INTENTIONALLY